NASA MEMO 10-10-58L

NASA

MEMORANDUM

EFFECT OF NOSE LENGTH, FUSELAGE LENGTH, AND NOSE FINENESS RATIO ON THE LONGITUDINAL AERODYNAMIC CHARACTERISTICS OF TWO COMPLETE MODELS AT HIGH SUBSONIC SPEEDS

By Kenneth W. Goodson

Langley Research Center
Langley Field, Va.

NATIONAL AERONAUTICS AND SPACE ADMINISTRATION

WASHINGTON

October 1958

NATIONAL AERONAUTICS AND SPACE ADMINISTRATION

NASA MEMO 10-10-58L

EFFECT OF NOSE LENGTH, FUSELAGE LENGTH, AND NOSE FINENESS RATIO ON THE LONGITUDINAL AERODYNAMIC CHARACTERISTICS OF TWO COMPLETE MODELS AT HIGH SUBSONIC SPEEDS

By Kenneth W. Goodson

SUMMARY

An investigation has been made of the effects of nose length, fuselage length, and nose fineness ratio on the static longitudinal aerodynamic characteristics of an airplane model with a swept wing and low tail and of a second model with a highly tapered wing of moderate sweep and a T-tail. The tests were conducted in the Langley high-speed 7- by 10-foot tunnel at Mach numbers from 0.60 to 0.92. The nose and body cross sections were circular.

For either the model with the swept wing and low tail or the model with the highly tapered wing of moderate sweep and the T-tail, the effects of forebody changes amounted primarily to rotations of the pitching-moment curves (changes in static margin) over the test ranges of angle of attack and Mach number. For the range of body shapes investigated the longitudinal stability at low lift is decreased by an increase in nose length or in fuselage length or by a reduction in nose fineness ratio when the fuselage length is held constant. In general, the stability for all model configurations showed substantially the same variation with changes in forebody area moment. The forebody changes did not alter the angle of attack at which an unstable break occurred in the moment contribution of the T-tail but did alter somewhat the magnitude of the instability.

INTRODUCTION

Experimental investigations of recent years (refs. 1 to 4) have shown that the aerodynamic characteristics of slender-fuselage airplane configurations (high-performance configurations) can be affected considerably by fuselage shape, length, and fineness ratio. The fuselage

geometric characteristics, in general, affect the cross flow, flow separation, and vortex formation on a configuration.

Since the flow phenomena occurring at the fuselage nose of forebody can influence the overall aerodynamic characteristics, the present investigation was undertaken to study the effects of nose length, fuselage length, and nose fineness ratio on the longitudinal aerodynamic characteristics of two complete model configurations, one representing a typical swept-wing design with a low tail, and the second representing a typical airplane with a highly tapered wing of moderate sweep and a high tail. Longitudinal stability data on models with the swept wing and on the highly tapered wing in combination with the basic fuselage (F_0) are presented in references 5 and 6, respectively.

The swept-wing model of the present investigation had a wing aspect ratio of 4.00, taper ratio of 0.30, and a quarter-chord sweep of 45° and was fitted with a chord plane horizontal tail. The highly tapered wing model had a wing aspect ratio of 3.00 with an unswept 0.80-chord line and was fitted with a high T-tail arrangement. Some data were obtained with the wings and tails removed from the model.

COEFFICIENTS AND SYMBOLS

The data are presented about the system of axes shown in figure 1. The pitching-moment coefficients are referred to a center-of-gravity position which is assumed to be located at the quarter-chord point of the mean aerodynamic chord of the wing under consideration. The force and moment coefficients of the various configurations are also based on the area, mean aerodynamic chord, and span of the wing under consideration.

C_L lift coefficient, $\frac{\text{Lift}}{qS}$

C_D drag coefficient, $\frac{\text{Drag}}{qS}$

C_m pitching-moment coefficient, $\frac{\text{Pitching moment}}{qS\bar{c}}$

ΔC_{m_t} pitching-moment increment due to the tail

ΔC_{m_α} incremental change in pitching-moment slope relative to that of the shortest nose length (F_3)

q	dynamic pressure, $\frac{\rho V^2}{2}$, lb/sq ft
ρ	mass density of air, slugs/cu ft
V	free-stream velocity, ft/sec
M	Mach number
S	wing area, sq ft
S_D	maximum cross-sectional area of fuselage, sq ft
c	local chord parallel to plane of symmetry, ft
$\bar{c}$	wing mean aerodynamic chord, $\frac{2}{S}\int_0^{b/2} c^2 dy$, ft
$\bar{c}_h$	horizontal-tail mean aerodynamic chord, ft
$\bar{c}_v$	vertical-tail mean aerodynamic chord, ft
b	wing span, ft
y	spanwise distance from plane of symmetry, ft
D	maximum diameter of fuselage, ft
α	angle of attack, deg
$\Lambda_{c/4}$	sweep of quarter-chord line, deg
R	radius of ogive nose, in.
M_N	moment of area of the various fuselage forebodies about assumed model center-of-gravity position, $in.^3$

Configuration components:

W	wing
F	fuselage
V	vertical tail

H horizontal tail

Subscripts:

0,1,2,3,4,5 various nose configurations (see fig. 3)

MODEL AND APPARATUS

A three-view drawing of the complete model with the 45° sweptback wing is shown in figure 2(a). This wing had an aspect ratio of 4.00, a taper ratio of 0.30, and was constructed of solid aluminum. The model was also fitted with a 45° sweptback horizontal tail located on the wing-chord plane.

A three-view drawing of the model having the highly tapered wing with zero sweep of the 0.80-chord line is shown in figure 2(b). The wing of this model was constructed of steel and had an aspect ratio of 3.00 and a taper ratio of 0.143. This model was fitted with a high horizontal tail (T-tail).

The vertical tail plan form was the same for both models, but the airfoil section was 9 percent thick for the swept-wing model and 6 percent thick for the highly tapered model. The incidence of the horizontal tails of both models was fixed at 0°.

The basic fuselage (F_0) was a body of revolution having a fineness ratio of 10.94 and an ogival nose. The dimensions of this body are presented in table I. The nose section of the basic fuselage was removable to allow testing of other nose lengths and nose fineness ratios. All nose sections were bodies of revolution. The pertinent dimensions of the various noses are shown in figure 3.

The nose-length series of bodies (fig. 3) were obtained by changing the nose fineness ratio and adding the various noses to the constant-length centerbody-afterbody portion of the fuselage. The fuselage length was varied by taking the smallest fineness ratio nose (shortest body length) and adding cylindrical sections to increase the overall fuselage length. The nose-fineness-ratio series was obtained by using the longest body in combination with the different fineness ratio noses.

TESTS

The sting-supported model was tested in the Langley high-speed 7- by 10-foot tunnel through a Mach number range of 0.60 to 0.92. The Reynolds number based on the mean aerodynamic chord of the models varied with Mach number from about 2.5×10^6 to 3.4×10^6.

Longitudinal stability tests were made for the swept-wing model and the highly tapered wing model with various nose lengths and nose fineness ratios. Tests were made of the complete model, wing-fuselage, body-tail, and body-alone configurations.

CORRECTIONS

Blockage corrections were applied to the results by the method of reference 7. Jet-boundary corrections to the angle of attack and drag were applied in accordance with reference 8. Corrections for effects of the longitudinal pressure gradient in the wind-tunnel test section have been applied to the data.

Model-support tares have not been applied, except for a fuselage base-pressure correction to the drag. The corrected drag data represent a condition of free-stream static pressure at the fuselage base. Past experience indicates that the influence of the sting support on the model characteristics is negligible with regard to the lift and pitching moment.

The angle of attack has been corrected for deflection of the balance and sting support. No attempt has been made to correct the data for aeroelastic distortion of the wings.

PRESENTATION OF RESULTS

The results of tests to determine the effects of nose length, fuselage length, and nose fineness ratio on the aerodynamic characteristics of the swept-wing model and the highly tapered wing model are presented in figures 4 to 14. (See the following table.)

Model	Tail	Configuration	Results	Figure
Swept wing	Low tail	Complete configuration	Basic longitudinal aerodynamic data	4
	Off	Wing-fuselage		5
	Low tail	Fuselage-tail		6
	Off	Fuselage alone		7
	Low tail	Complete model	$\partial C_m/\partial C_L$	8
	Low tail	Complete model and fuselage-tail	ΔC_{m_t}	9
Highly tapered wing	T-tail	Complete model	Basic longitudinal aerodynamic data	10
	Off	Wing-fuselage		11
	T-tail	Fuselage-tail		12
	Off	Fuselage alone		13
	T-tail	Complete model and fuselage-tail	ΔC_{m_t}	14
		Correlation of all nose configurations	$\Delta C_{m_\alpha}\left(\frac{S\bar{c}}{S_D D}\right)$ plotted against Nose moment of area	15

DISCUSSION

Swept Wing and Low Tail

Nose length.- The principal effect of increasing the nose length of the complete model by increasing the nose fineness ratio (fig. 4(a)) was to reduce the longitudinal stability through the lift range. (See fig. 8.) Study of the lift results (fig. 4(c)) and the pitching-moment data (figs. 4(a) and (b)) indicates that in changing to the longest nose (WF_1VH), the center of load is not moved as far forward as might be expected from the increase in length alone, presumably because of the

change in nose shape (higher fineness ratio). These trends are still evident when the tail is removed from the model (fig. 5), when the wing is removed (body-tail configuration, fig. 6), and for the fuselage alone (fig. 7). Comparison of the wing-on and wing-off tail pitching-moment increments (figs. 9(a) and (b)) indicates that the presence of the wing reduces the effects of nose length on the tail contribution to the pitching moment at $M = 0.80$ primarily at the higher angles of attack; however, at $M = 0.90$, the shortest nose produces a rather erratic effect with wing on.

Fuselage length.- Increasing the fuselage length by adding cylindrical inserts to the center section of the fuselage and keeping the blunt-nose shape (F_3, fig. 3) results in a reduction in longitudinal stability similar to but greater than that obtained when the change in length is made by an increase in nose fineness ratio. (See figs. 4 and 8.) A comparison of these two sets of data (fig. 4(c)) shows that the nose with cylindrical inserts tends to carry more lift than the high fineness ratio noses.

Similar results are obtained when the tail, wing, or both are removed from the fuselage (figs. 5, 6, and 7, respectively); however, the lift increment tends to be more nearly proportional to the increase in fuselage length than that obtained on the complete configuration, which again indicates that the wing-on and tail-on characteristics are somewhat affected by the nose-generated flow field. Comparison of the tail pitching-moment increments given in figure 9 with wing-on and wing-off shows further evidence of some slight effect of nose-generated flow field on the tail.

Nose fineness ratio.- When the nose fineness ratio of the body was increased by slenderizing the nose of the longest body, increases in longitudinal stability resulted. This is in contrast to the reduction in stability noted previously when an increase in nose fineness ratio was achieved by extending the nose length. The present result may be explained by the fact that increasing the nose fineness ratio on a constant-length body shifts the lift center rearward due to the change in nose shape and lifting area. These trends are also evident with the tail removed (fig. 5), with the wing removed (fig. 6), and with the body alone (fig. 7). Study of the tail pitching-moment increments of these configurations (nose-fineness-ratio series, fig. 9) seems to indicate that the wing reduces the effect of nose wake on the low tail of the swept-wing model. The erratic curve obtained with the shortest length nose of the nose length series at $M = 0.90$ (fig. 9) is eliminated when this shape is added to the longest body (nose-fineness-ratio series), indicating that the forebody length controls somewhat the vertical position of the nose wake and its influence on the tail.

Highly Tapered Wing and T-Tail

The incremental effects of nose length, fuselage length, and nose fineness ratio on the pitching moments for the highly tapered wing model are basically very similar to those obtained on the swept-wing model. (See figs. 10 and 11.) The difference in the basic shape of the pitching-moment curves for the two complete models is due primarily to the wing plan form and tail position used. The swept-wing plan form usually shows a tendency toward longitudinal instability at low lifts and low angles of attack as is seen in figure 5, with the low tail tending to minimize this tendency and also to cause a nose-dowm moment at the higher (near stall) angles of attack (fig. 4). The highly tapered wing tends to eliminate the tail-off instability at the higher angles of attack (fig. 11). Addition of a T-tail results in instability just beyond wing stall as is shown in figures 10(a) and (b).

The changes in the aerodynamic results of the highly tapered wing due to the nose length and shape are similar to those obtained with the swept-wing model (figs. 10 to 13). The incremental contribution of the T-tail to the pitching-moment curves appears to be influenced predominately by the variation of wing-wake characteristics with angle of attack. The effects of forebody shape were relatively small (fig. 14). With any of the forebodies, the unstable break in the pitching-moment curve occurred at essentially the same angle of attack, although the magnitude of the instability was affected somewhat by forebody shape. The changes in lift and drag due to change in nose shape or length with either the high or low tail configurations were generally small.

Correlation of Nose Effects

A review of the preceding sections indicates that variations in pitching-moment-curve slopes are associated with changes in forebody area and center of load. Consequently, a correlation showing the variation of pitching-moment-curve-slope increments with forebody moment of area was made. The slope increments were obtained by subtracting the value for the shortest length nose from those of the other noses. These slope increments were then reduced to a common reference based on the fuselage area and diameter. The nose moments of area (area forward of the moment reference center) were measured about the assumed model center of gravity. The correlation (fig. 15) shows that $\Delta C_{m_\alpha}\left(\frac{S\bar{c}}{S_D D}\right)$ is primarily affected by the moment of area with the scatter in points being due to secondary effects. In general, substantially the same rate of change in the moment-slope parameter with change in forebody area moment is obtained for all model configurations.

CONCLUSIONS

The results of a wind-tunnel investigation at high subsonic speeds of the effects of nose length, fuselage length, and nose fineness ratio for complete models representative of a typical design with a swept wing and low tail and of a typical design with a highly tapered wing of moderate sweep and a T-tail indicate the following conclusions:

1. For either the model with the swept wing and low tail or the model with the highly tapered wing and T-tail, the effects of forebody changes amounted primarily to rotations of the pitching-moment curves (changes in static margin) over the test ranges of angle of attack and Mach number.

2. For the range of body shapes investigated, the longitudinal stability at low lift is decreased by an increase in nose length or in fuselage length or by a reduction in nose fineness ratio when the fuselage length is held constant. In general, the stability for all model configurations showed substantially the same variation with changes in forebody area moment.

3. The forebody changes did not alter the angle of attack at which an unstable break occurred in the moment contribution of the T-tail but did alter somewhat the magnitude of the instability.

Langley Research Center,
National Aeronautics and Space Administration,
Langley Field, Va., April 29, 1958.

REFERENCES

1. Kuhn, Richard E., Hallissy, Joseph M., Jr., and Stone, Ralph W., Jr.: A Discussion of Recent Wind-Tunnel Studies Relating to the Problem of Estimating Vertical- and Horizontal-Tail Loads. NACA RM L55E16a, 1955.

2. Jaquet, Byron M., and Fletcher, H. S.: Effects of Fuselage Nose Length and a Canopy on the Static Longitudinal and Lateral Stability Characteristics of 45° Sweptback Airplane Models Having Fuselages With Square Cross Sections. NACA TN 3961, 1957.

3. Goodman, Alex, and Thomas, David F., Jr.: Effects of Wing Position and Fuselage Size on the Low-Speed Static and Rolling Stability Characteristics of a Delta-Wing Model. NACA Rep. 1224, 1955. (Supersedes NACA TN 3063.)

4. Polhamus, Edward C.: Effect of Nose Shape on Subsonic Aerodynamic Characteristics of a Body of Revolution Having a Fineness Ratio of 10.94. NACA RM L57F25, 1957.

5. Goodson, Kenneth W., and Becht, Robert E.: Wind-Tunnel Investigation at High Subsonic Speeds of the Stability Characteristics of a Complete Model Having Sweptback-, M-, W-, and Cranked-Wing Plan Forms and Several Horizontal-Tail Locations. NACA RM L54C29, 1954.

6. Goodson, Kenneth W.: Static Longitudinal Characteristics at High Subsonic Speeds of a Complete Airplane Model With a Highly Tapered Wing Having the 0.80 Chord Line Unswept and With Several Tail Configurations. NACA RM L56J03, 1957.

7. Herriot, John G.: Blockage Corrections for Three-Dimensional-Flow Closed-Throat Wind Tunnels, With Consideration of the Effect of Compressibility. NACA Rep. 995, 1950. (Supersedes NACA RM A7B28.)

8. Gillis, Clarence L., Polhamus, Edward C., and Gray, Joseph L., Jr.: Charts for Determining Jet-Boundary Corrections for Complete Models in 7- by 10-Foot Closed Rectangular Wind Tunnels. NACA WR L-123, 1945. (Formerly NACA ARR L5G31.)

TABLE I.- FUSELAGE ORDINATES

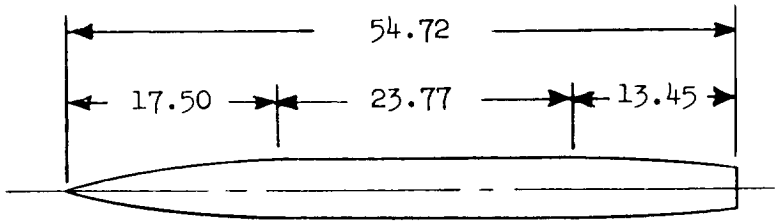

Station, in.	Radius, in.
0	0
2.00	.53
4.00	1.00
6.00	1.44
8.00	1.80
10.00	2.07
12.00	2.30
14.00	2.42
16.00	2.47
17.50	2.50
41.27	2.50
43.27	2.42
45.27	2.35
47.27	2.25
48.30	2.14
54.72	1.65

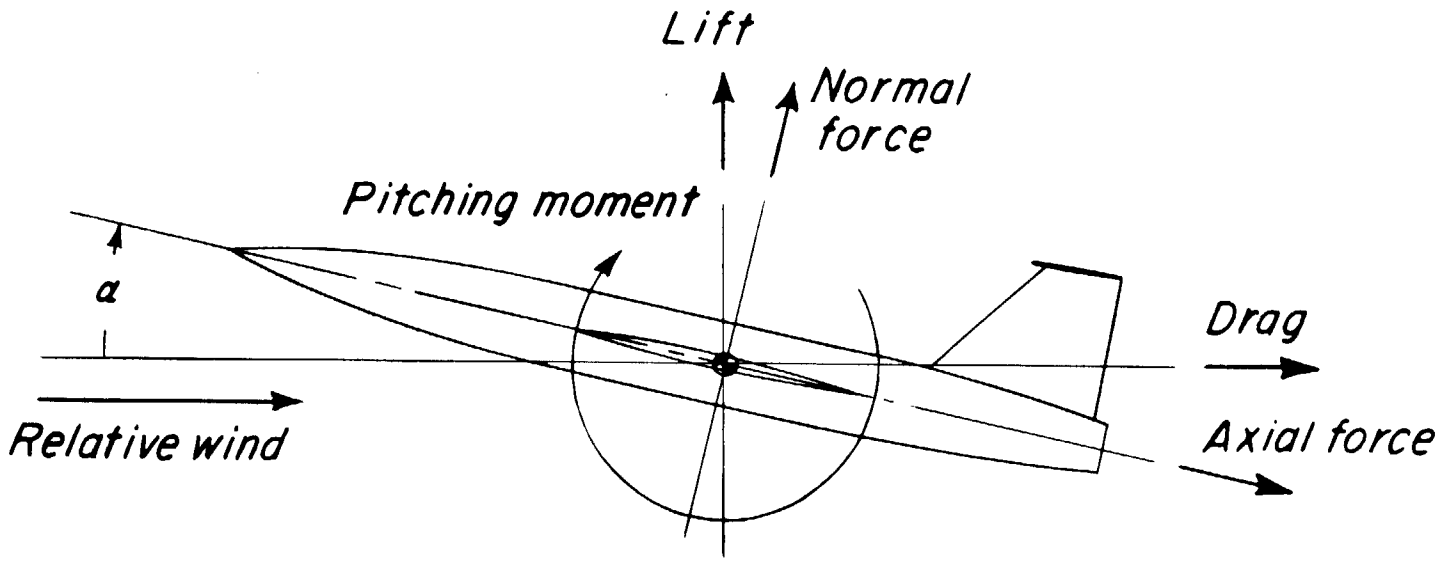

Figure 1.- System of axes (positive values of forces, moments, and angles are indicated by arrows).

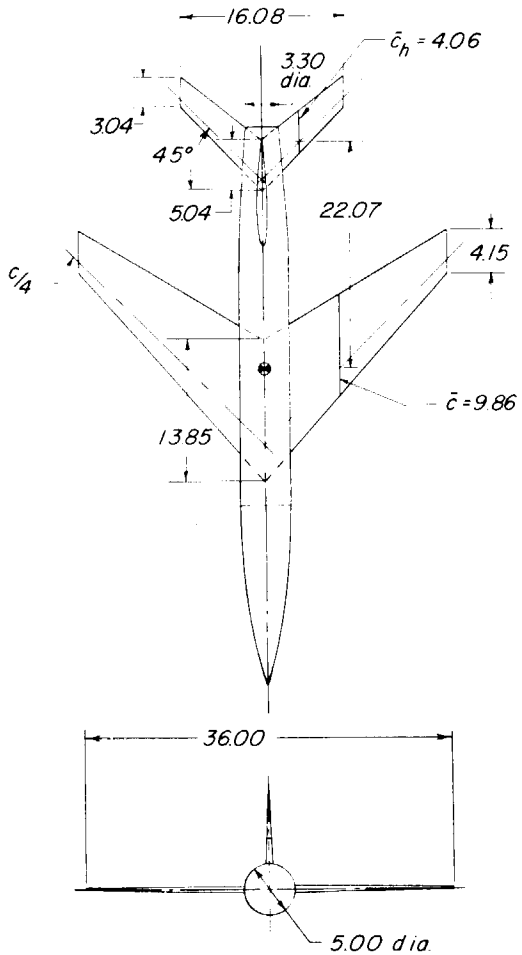

Geometric Characteristics Of Model			
	Wing	Horiz. tail	Vert. tail
Area, ft^2	2.25	.451	.612
Aspect ratio	4.00	3.98	1.18
Taper ratio	.30	.603	.411
$\Lambda_{c/4}$, deg	45	45	28.39
NACA airfoil section parallel to airstream	65A006	65A006	65A009

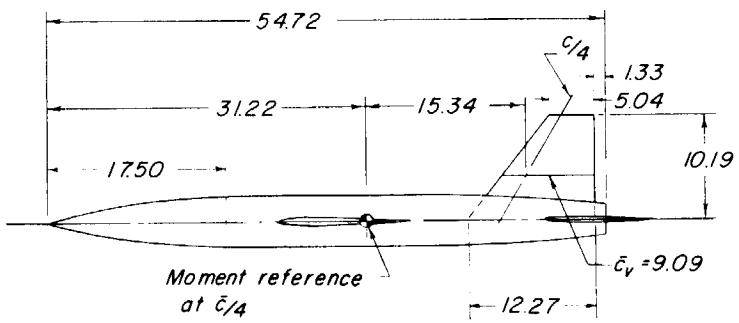

(a) Swept-wing model.

Figure 2.- Geometric characteristics of the two complete models. All dimensions are in inches.

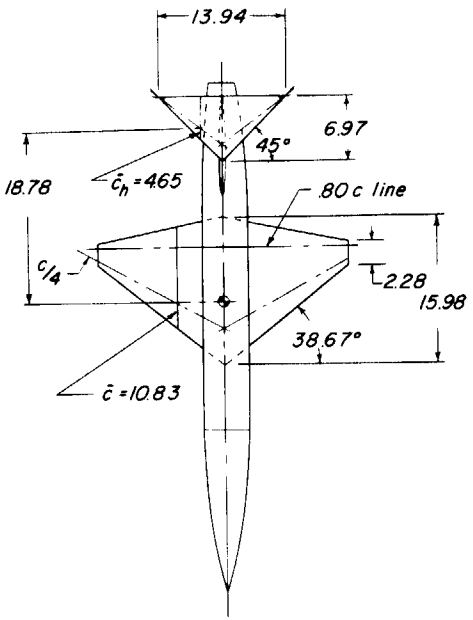

Geometric Characteristics Of Model			
	Wing	Horiz. tail	Vert. tail
Area, ft^2	1.74	.337	.603
Aspect ratio	3.00	4.00	1.16
Taper ratio	.143	0	.411
$\Lambda_{c/4}$, deg	28.82	36.85	28.39
NACA airfoil section parallel to airstream	65A004	65A006	65A006

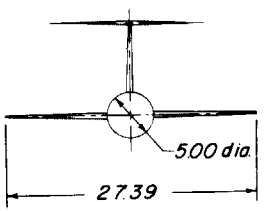

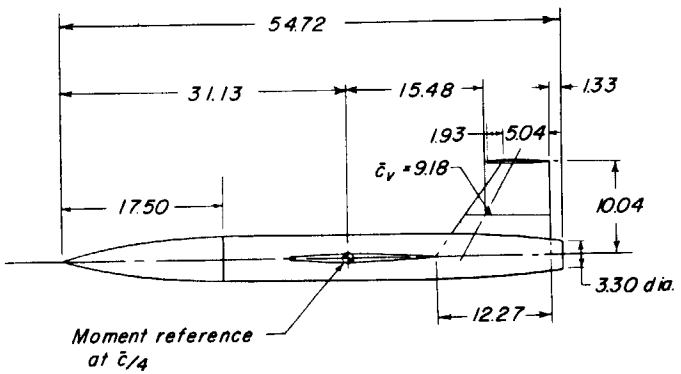

(b) Highly tapered wing model.

Figure 2.- Concluded.

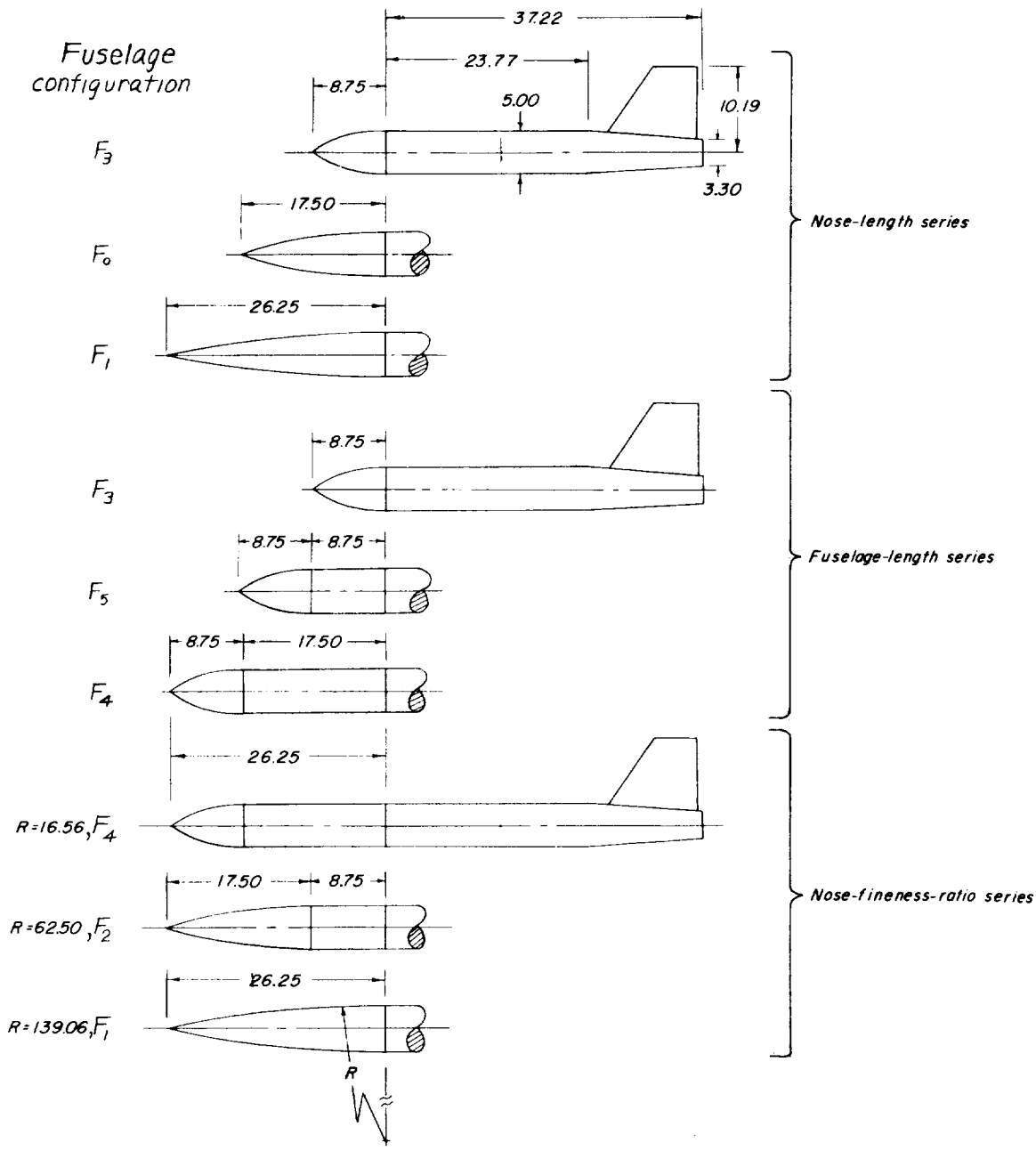

Figure 3.- Various nose configurations tested on the swept and highly tapered wing models.

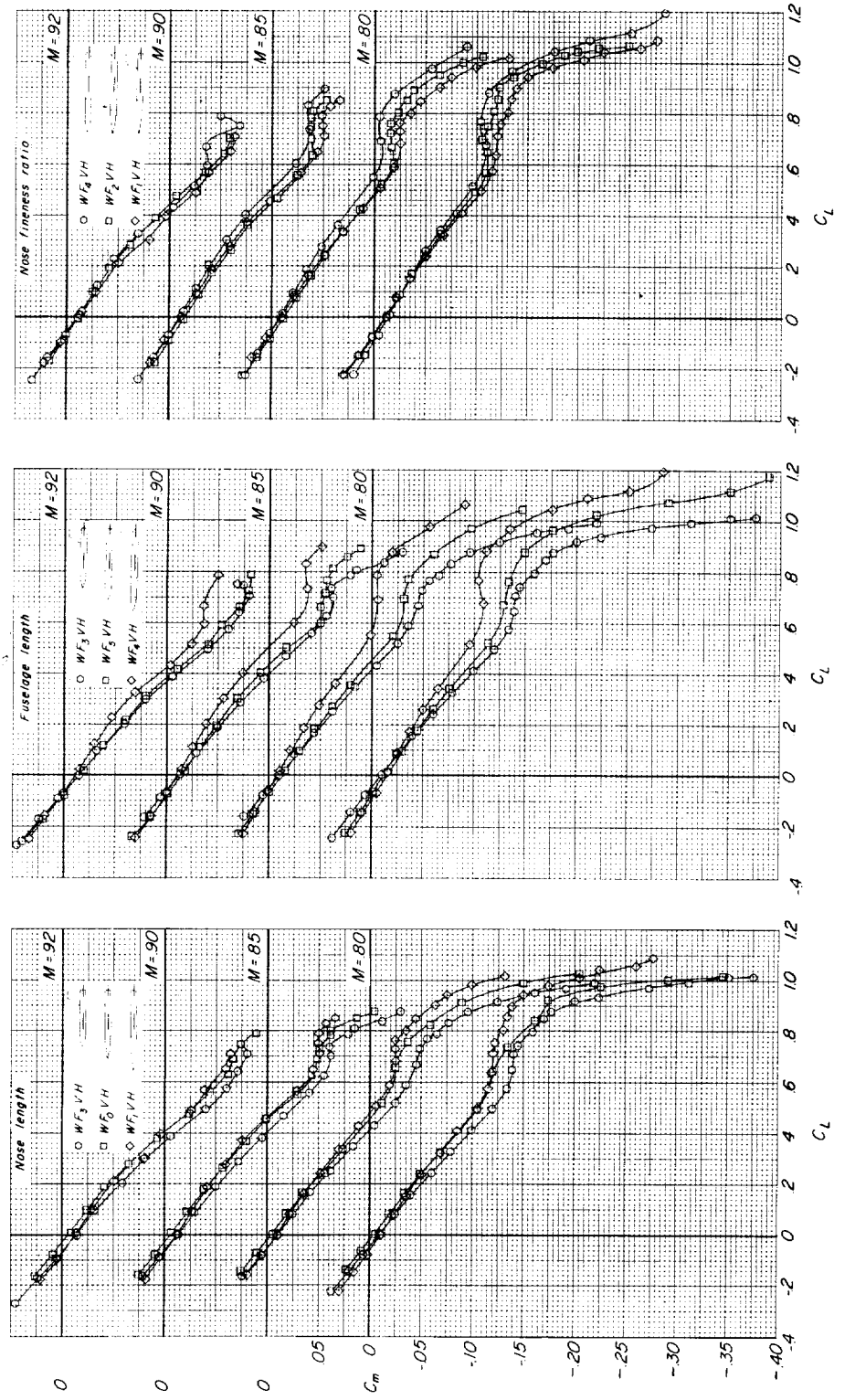

(a) C_m against C_L.

Figure 4.- Effect of nose length, fuselage length, and nose fineness ratio on the longitudinal aerodynamic characteristics of a complete swept-wing model. Low tail.

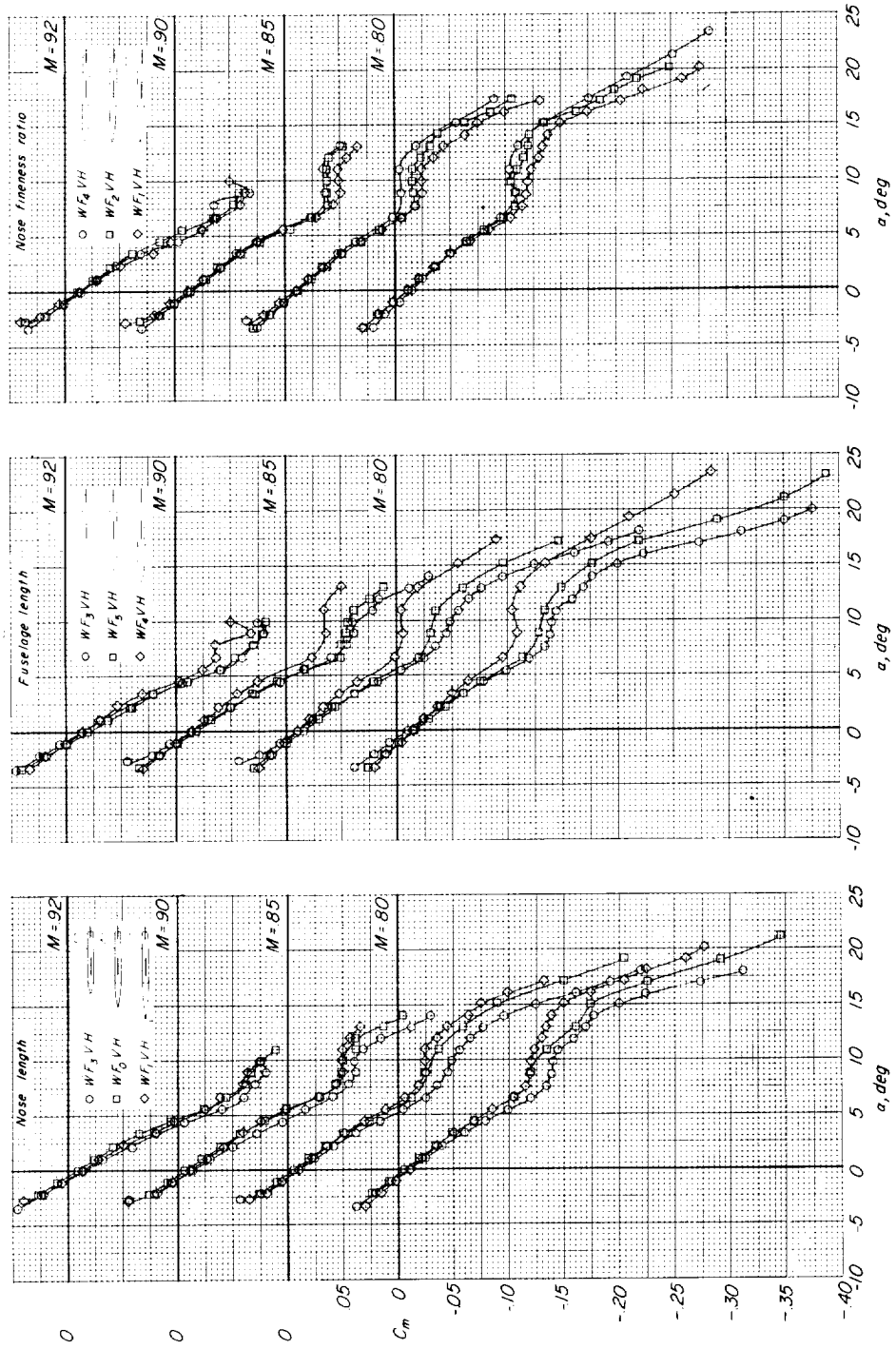

(b) C_m against α.

Figure 4.- Continued.

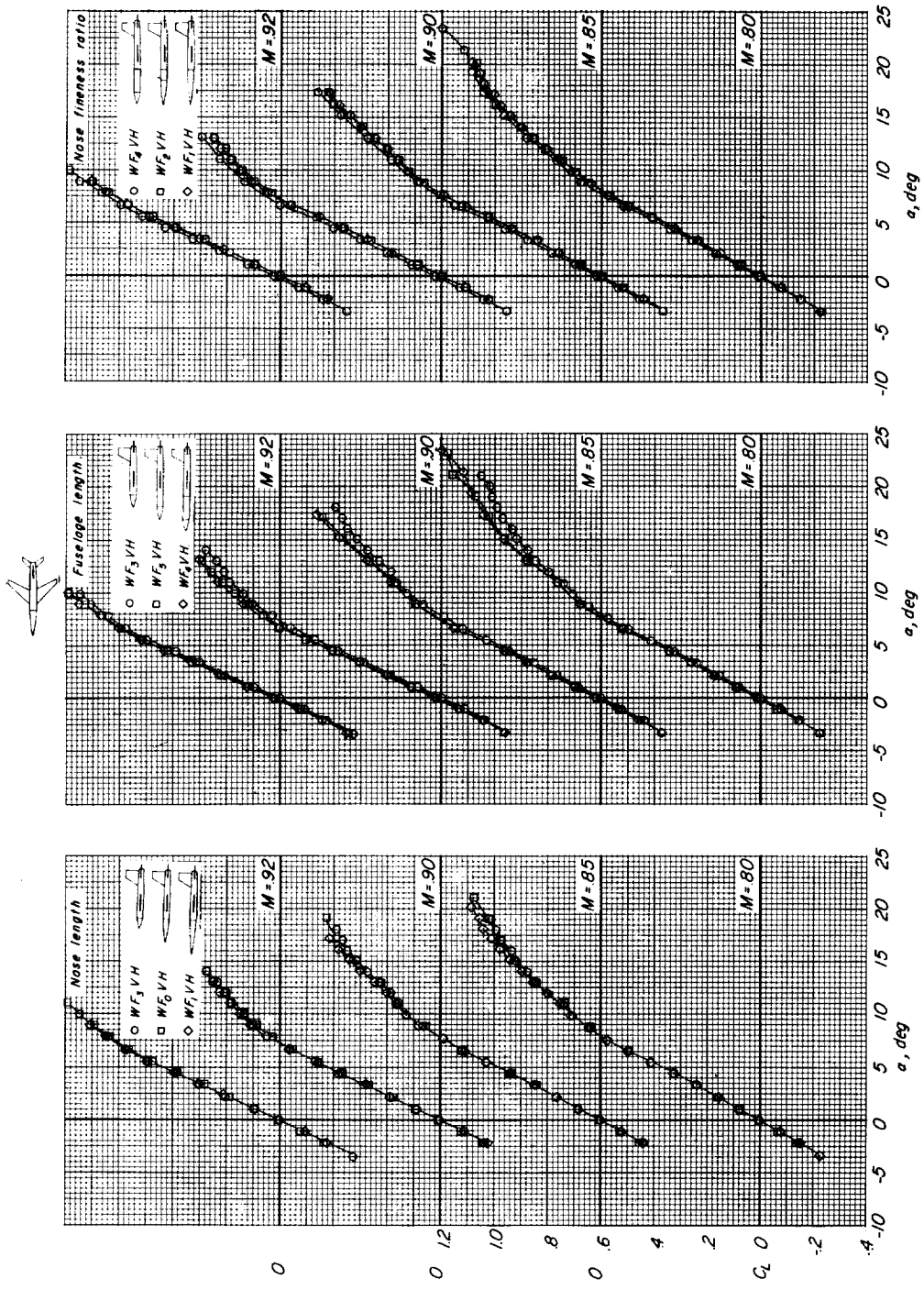

(c) C_L against α.

Figure 4.- Continued.

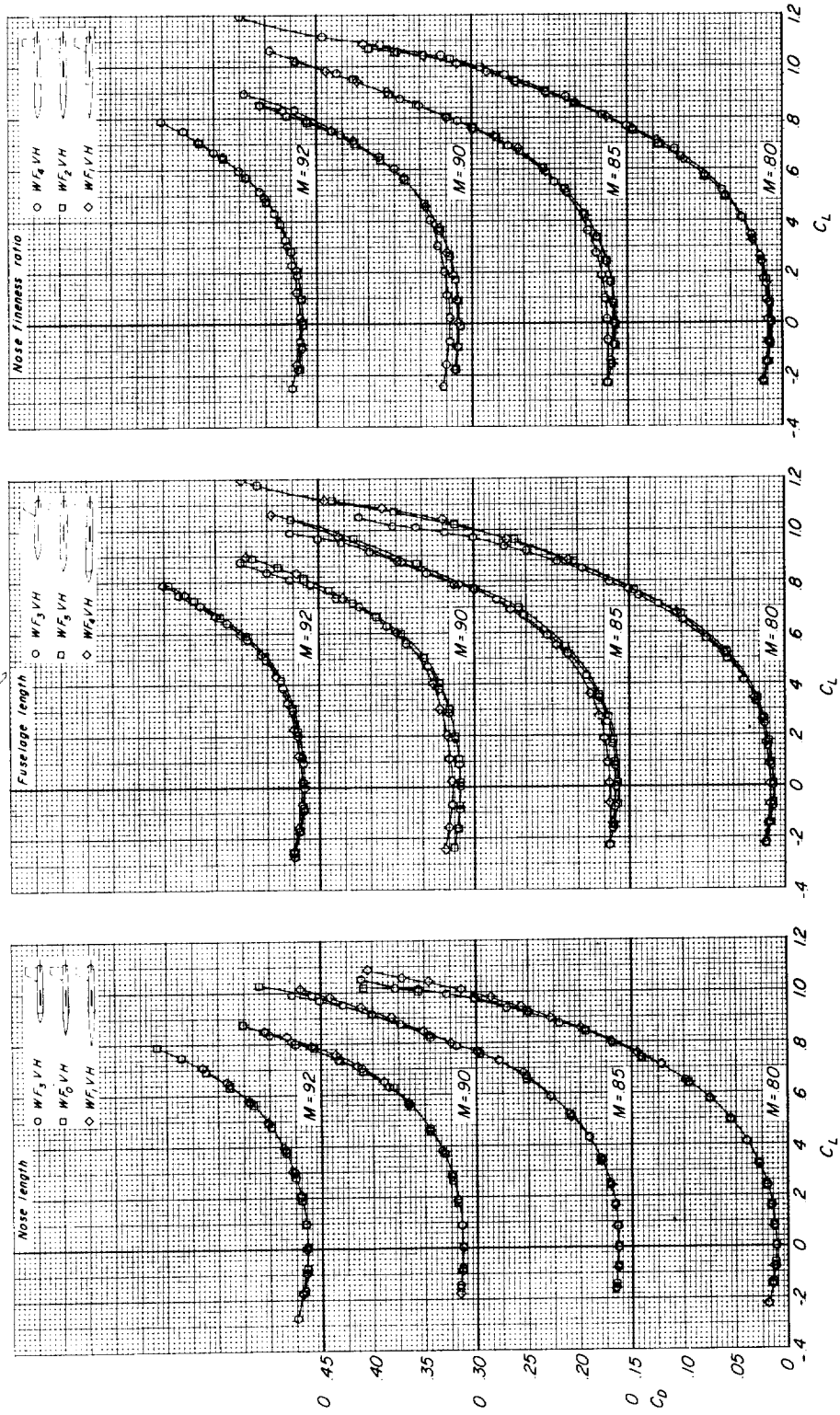

(d) C_D against C_L.

Figure 4.- Continued.

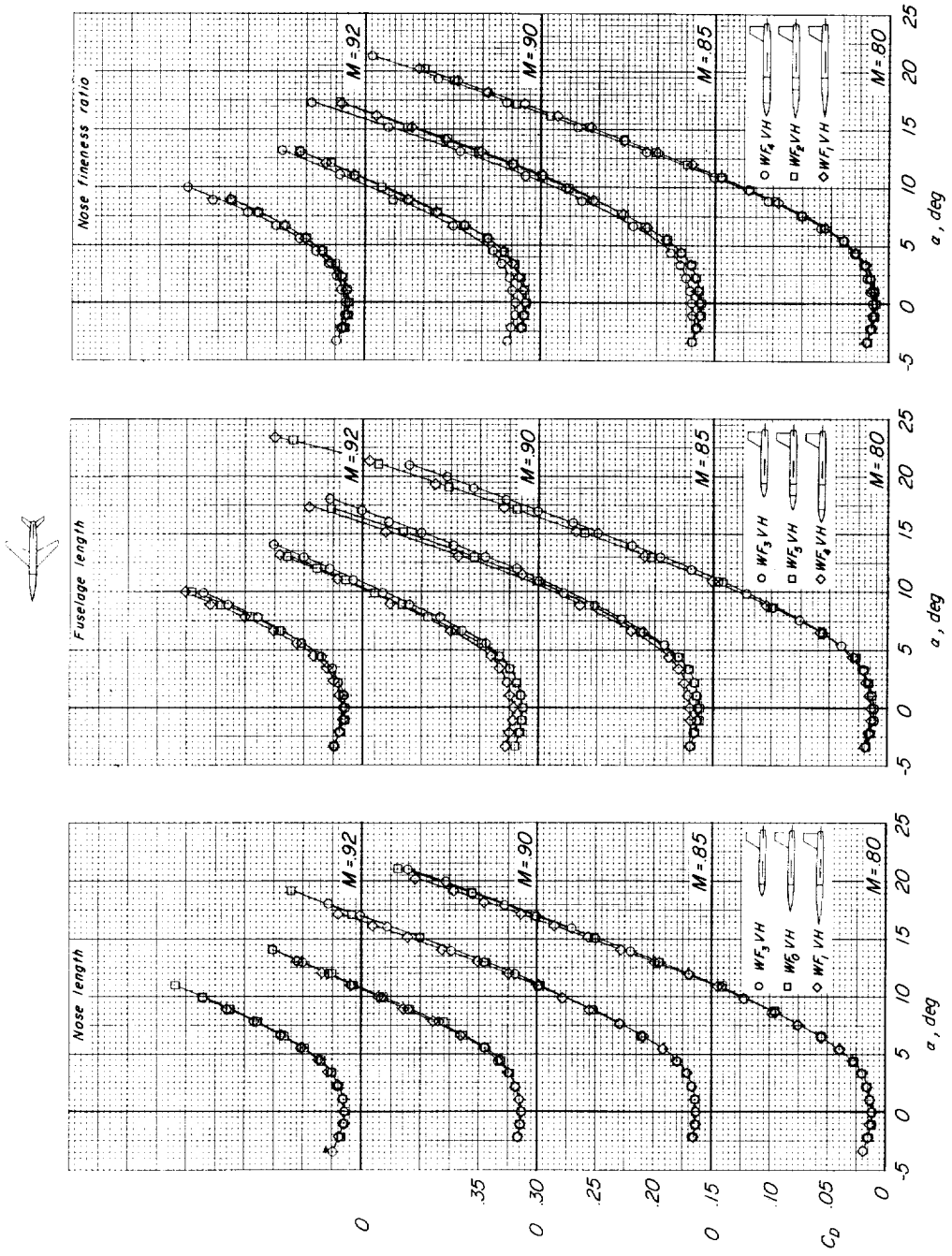

(e) C_D against α.

Figure 4.- Concluded.

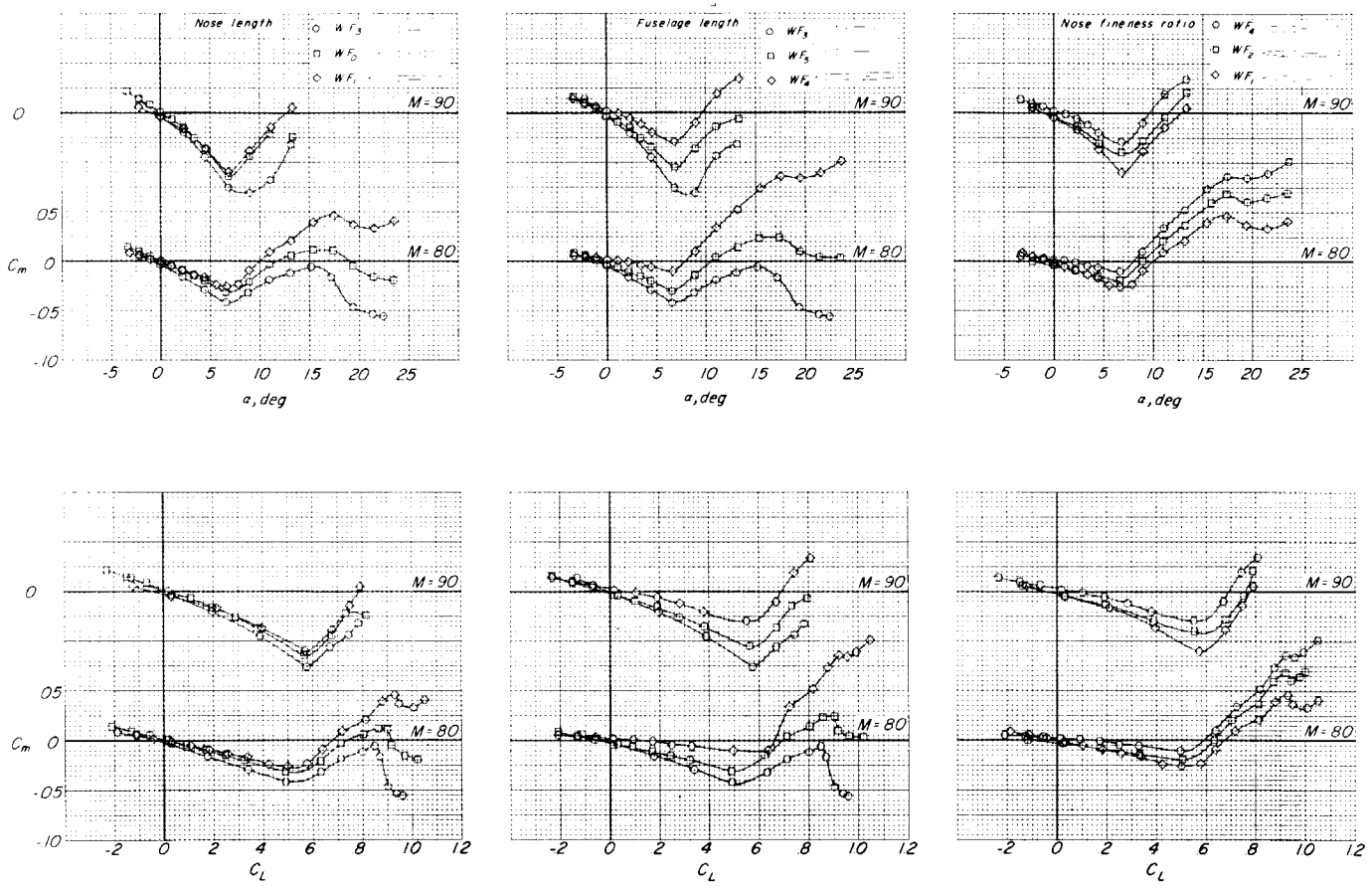

(a) C_m against α and C_L.

Figure 5.- Effect of nose length, fuselage length, and nose fineness ratio on the longitudinal aerodynamic characteristics of a swept-wing model. Tail off.

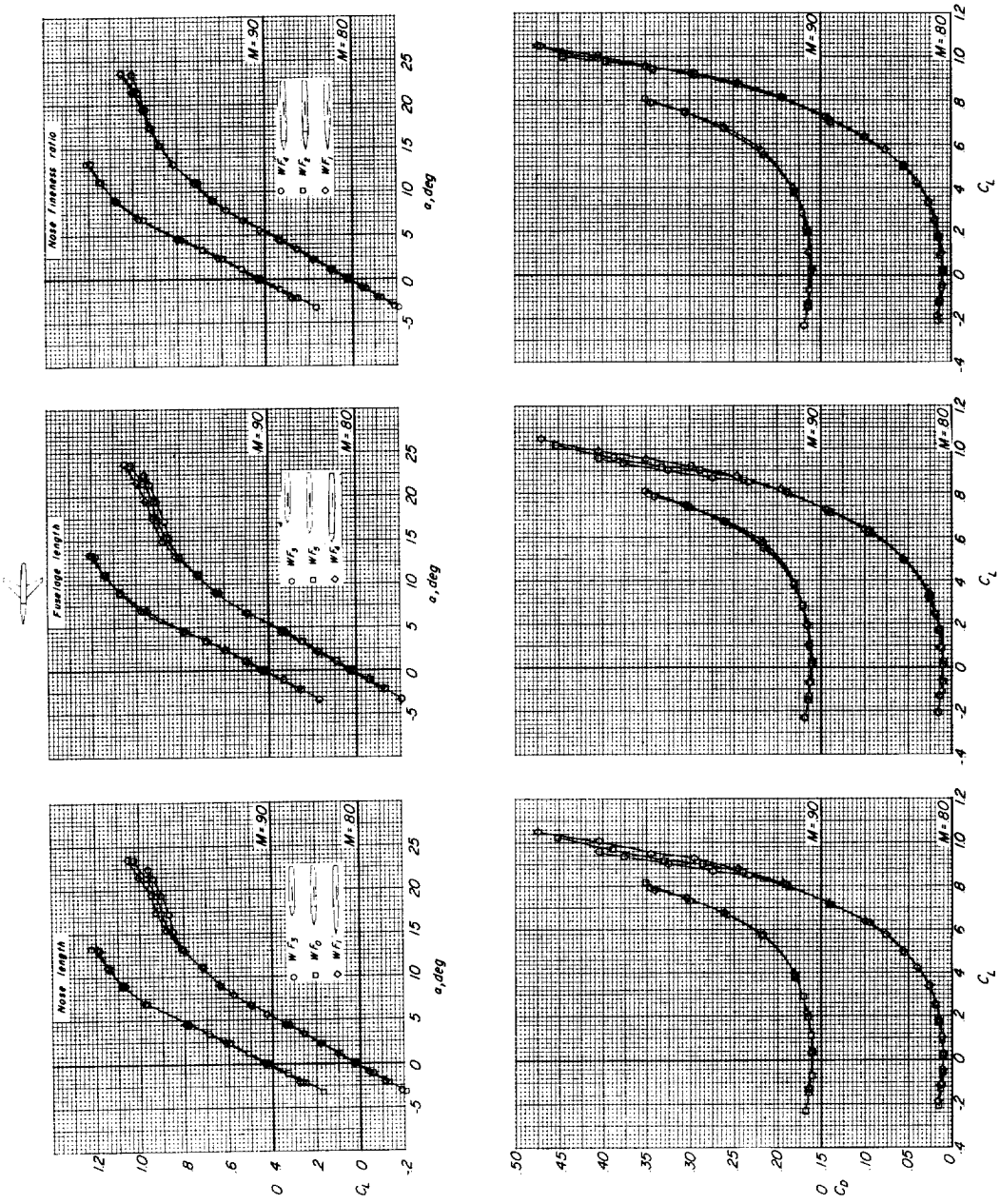

(b) C_L against α and C_D against C_L.

Figure 5.- Continued.

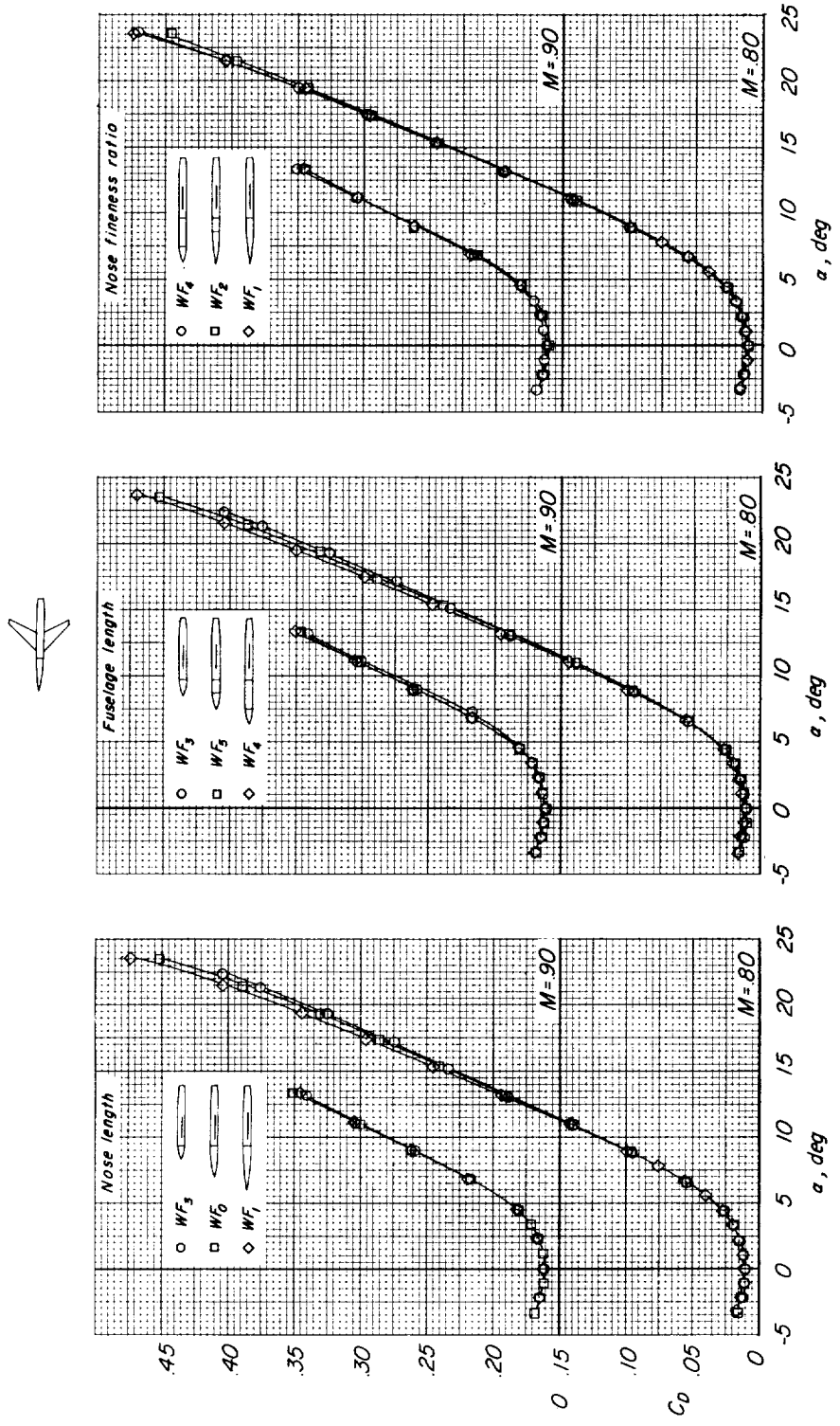

(c) C_D against α.

Figure 5.- Concluded.

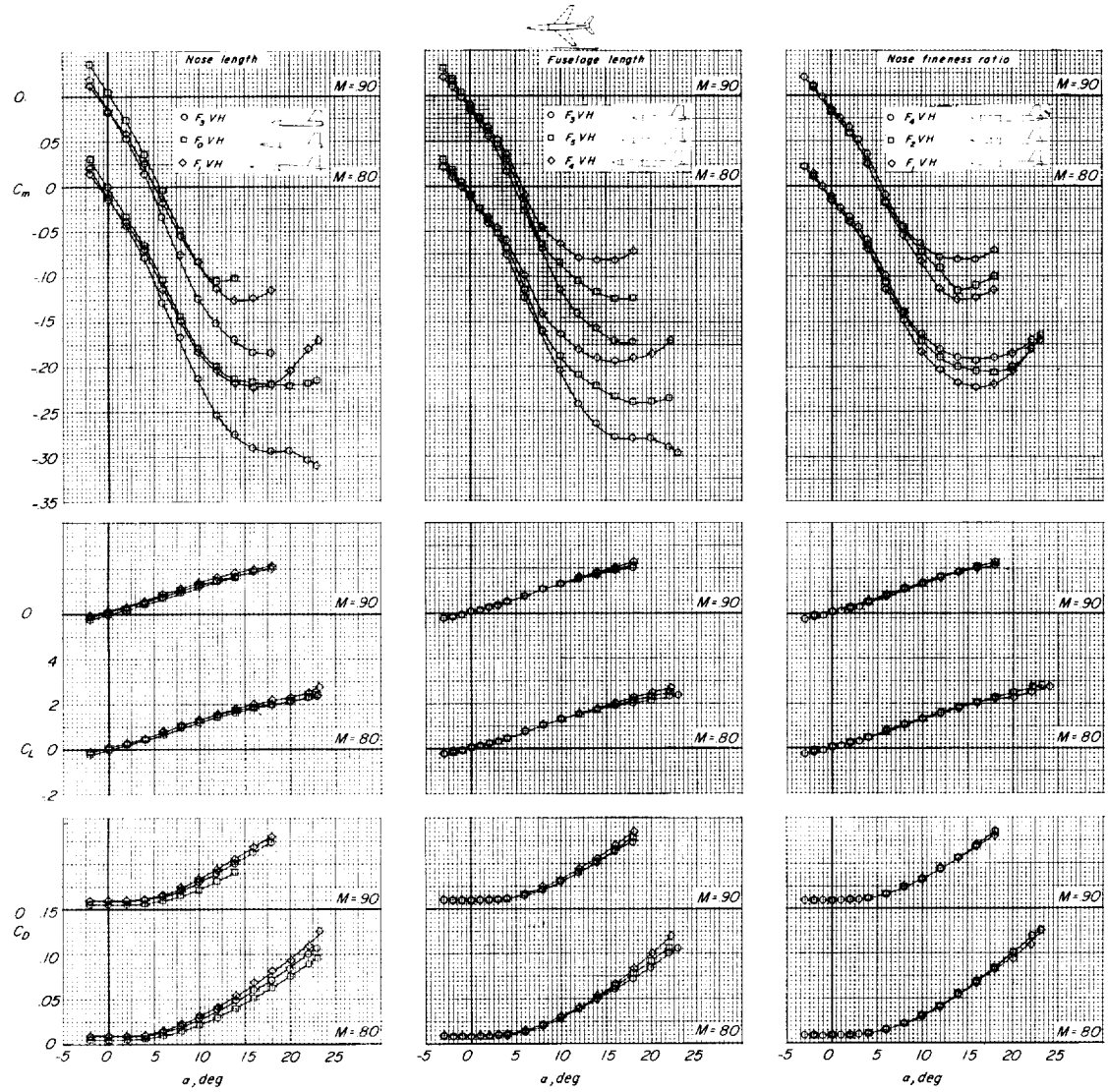

Figure 6.- Effect of nose length, fuselage length, and nose fineness ratio on the longitudinal aerodynamic characteristics of the fuselage and tail of the swept-wing model. Low tail.

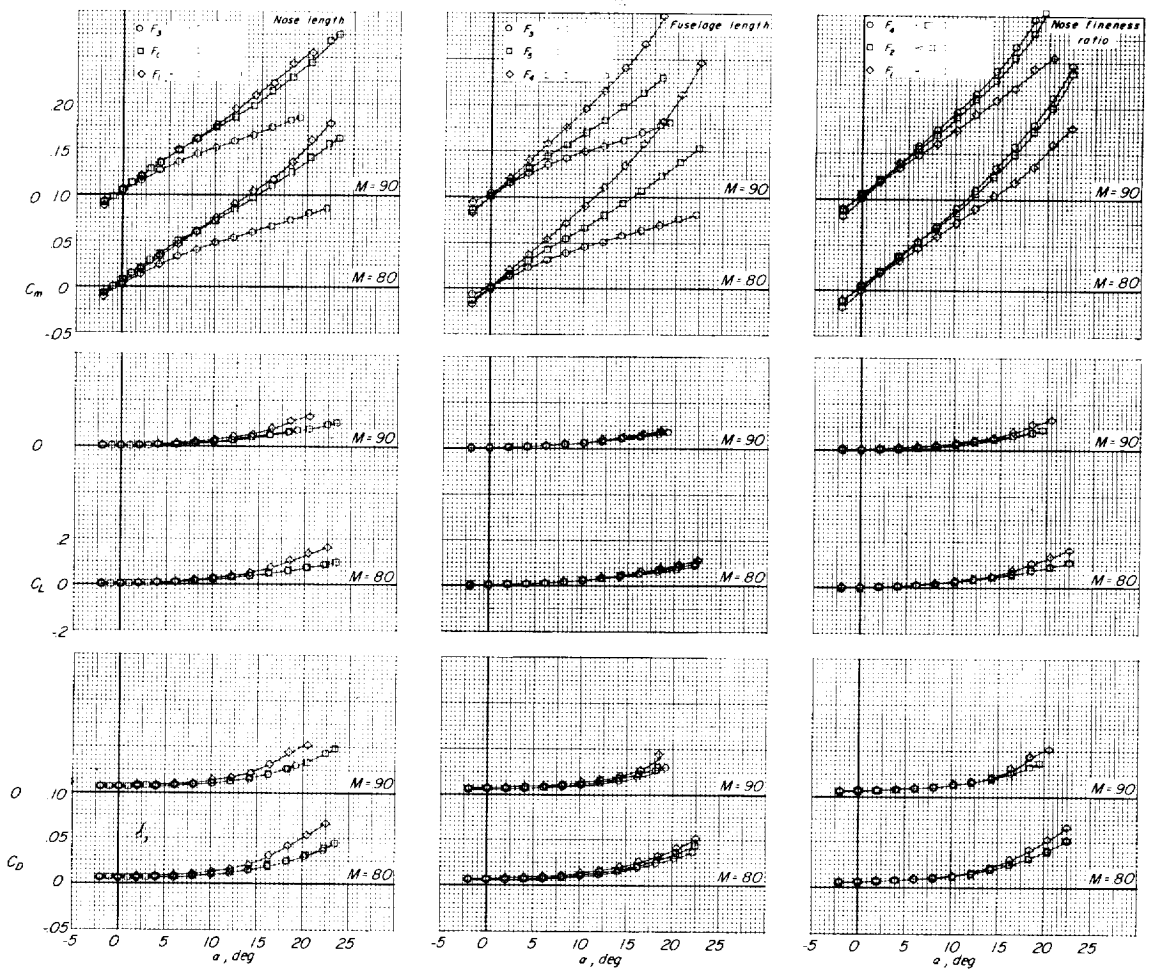

Figure 7.- Effect of nose length, fuselage length, and nose fineness ratio on the longitudinal aerodynamic characteristics of the fuselage of the swept-wing model.

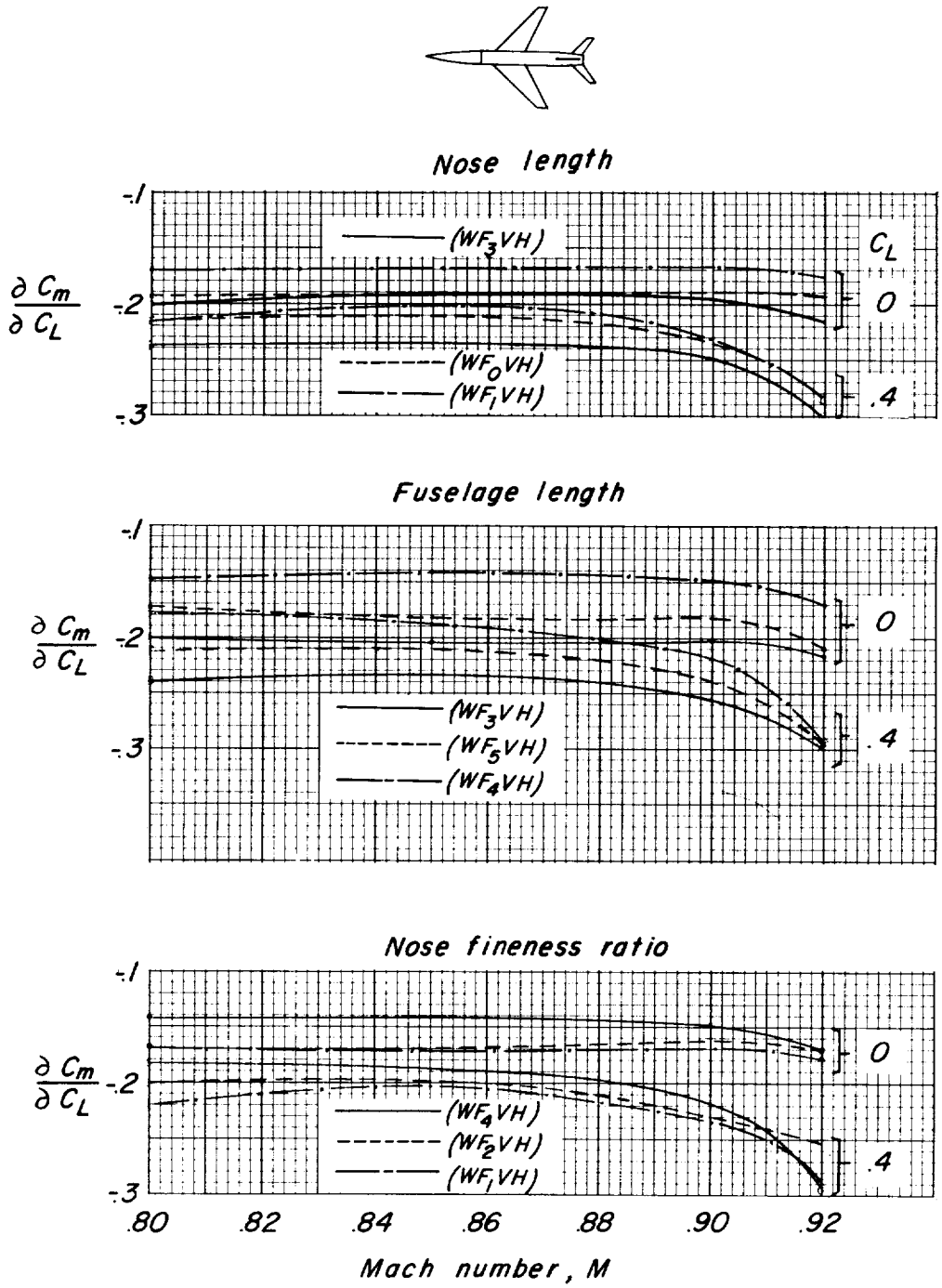

Figure 8.- Variation of $\partial C_m/\partial C_L$ with Mach number for the complete swept-wing model with various nose configurations. Low tail.

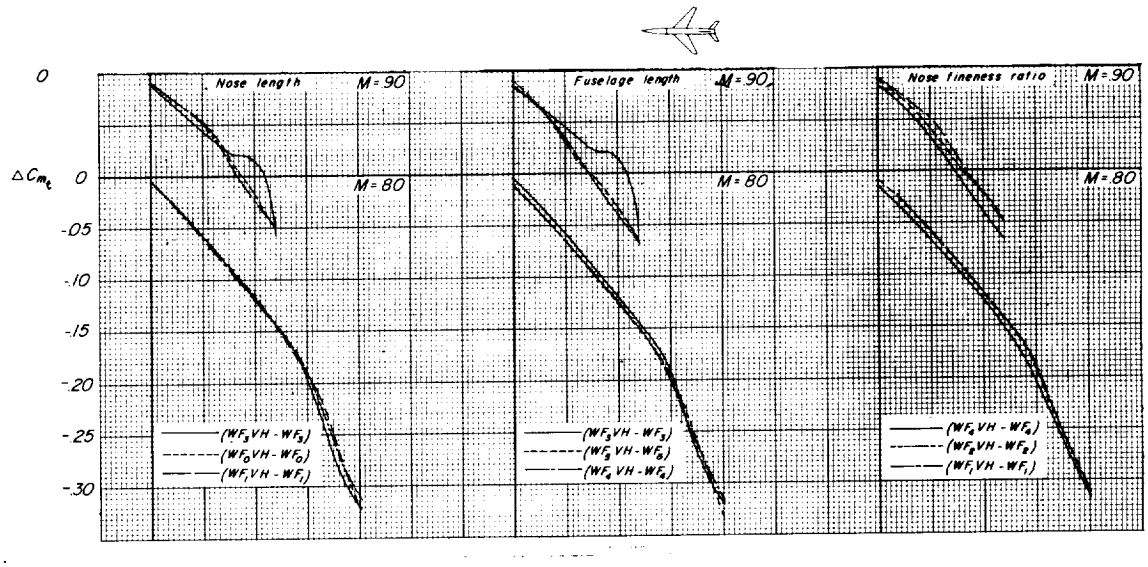

(a) Wing on.

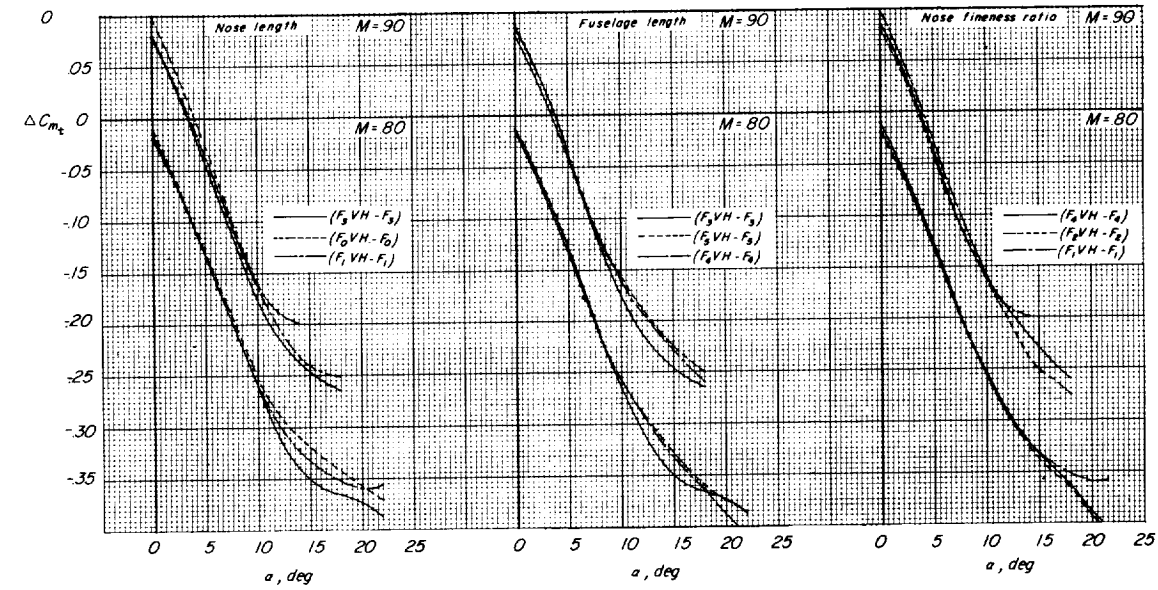

(b) Wing off.

Figure 9.- Effect of nose length, fuselage length, and nose fineness ratio on the tail contribution to the swept-wing model. Low tail.

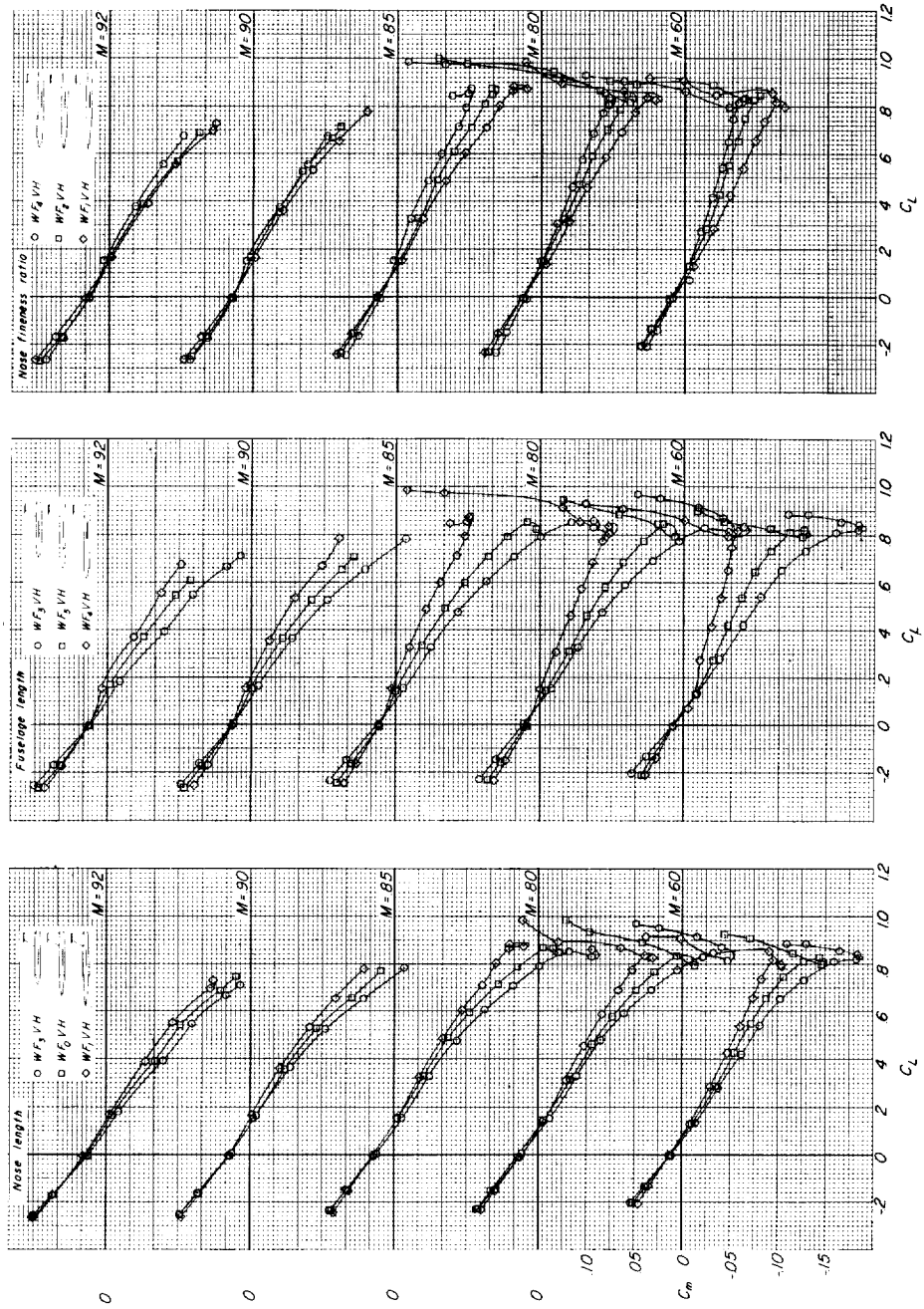

(a) C_m against C_L.

Figure 10.- Effect of nose length, fuselage length, and nose fineness ratio on the longitudinal aerodynamic characteristics of a complete model with highly tapered wing. T-tail.

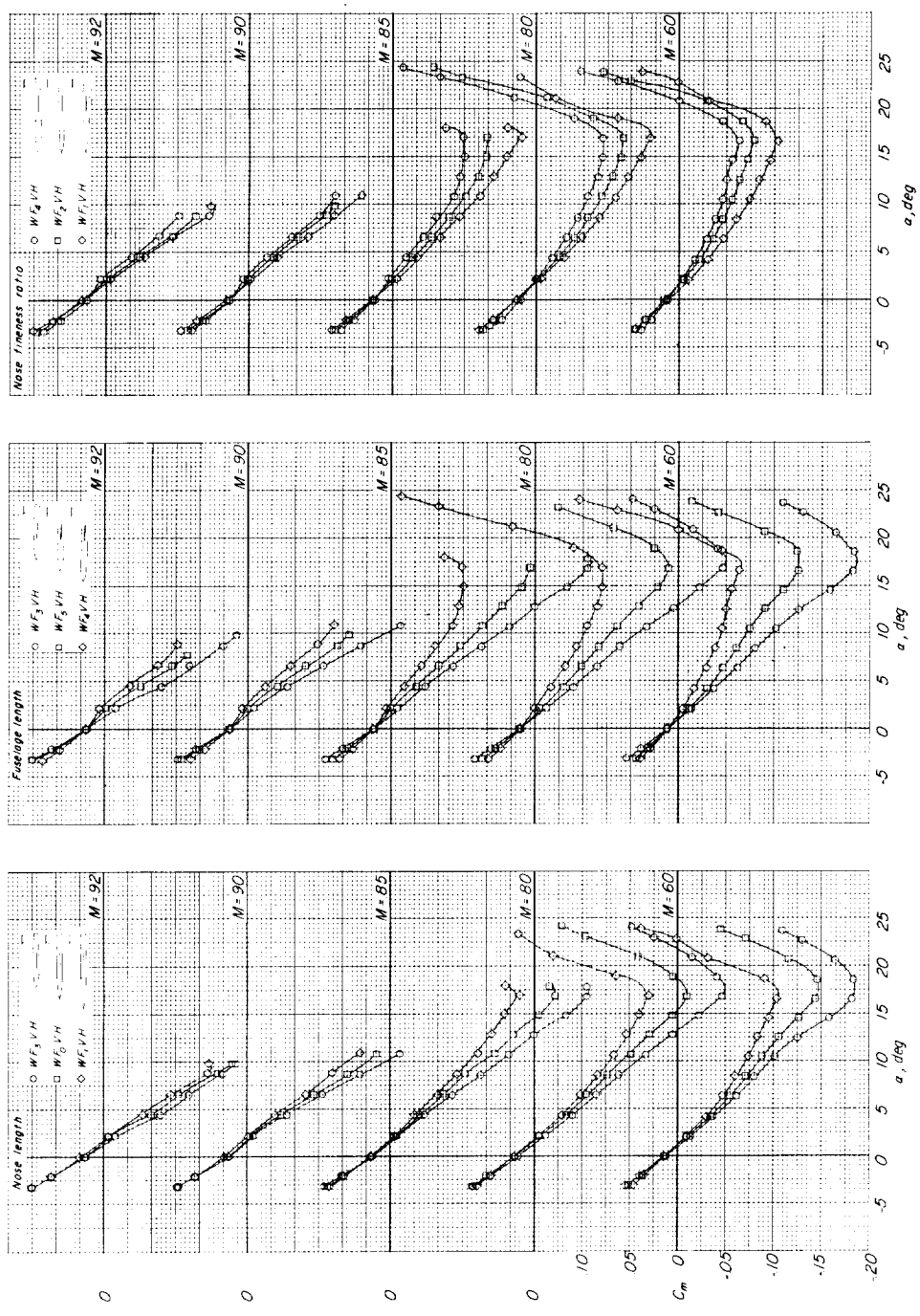

(b) C_m against α.

Figure 10.- Continued.

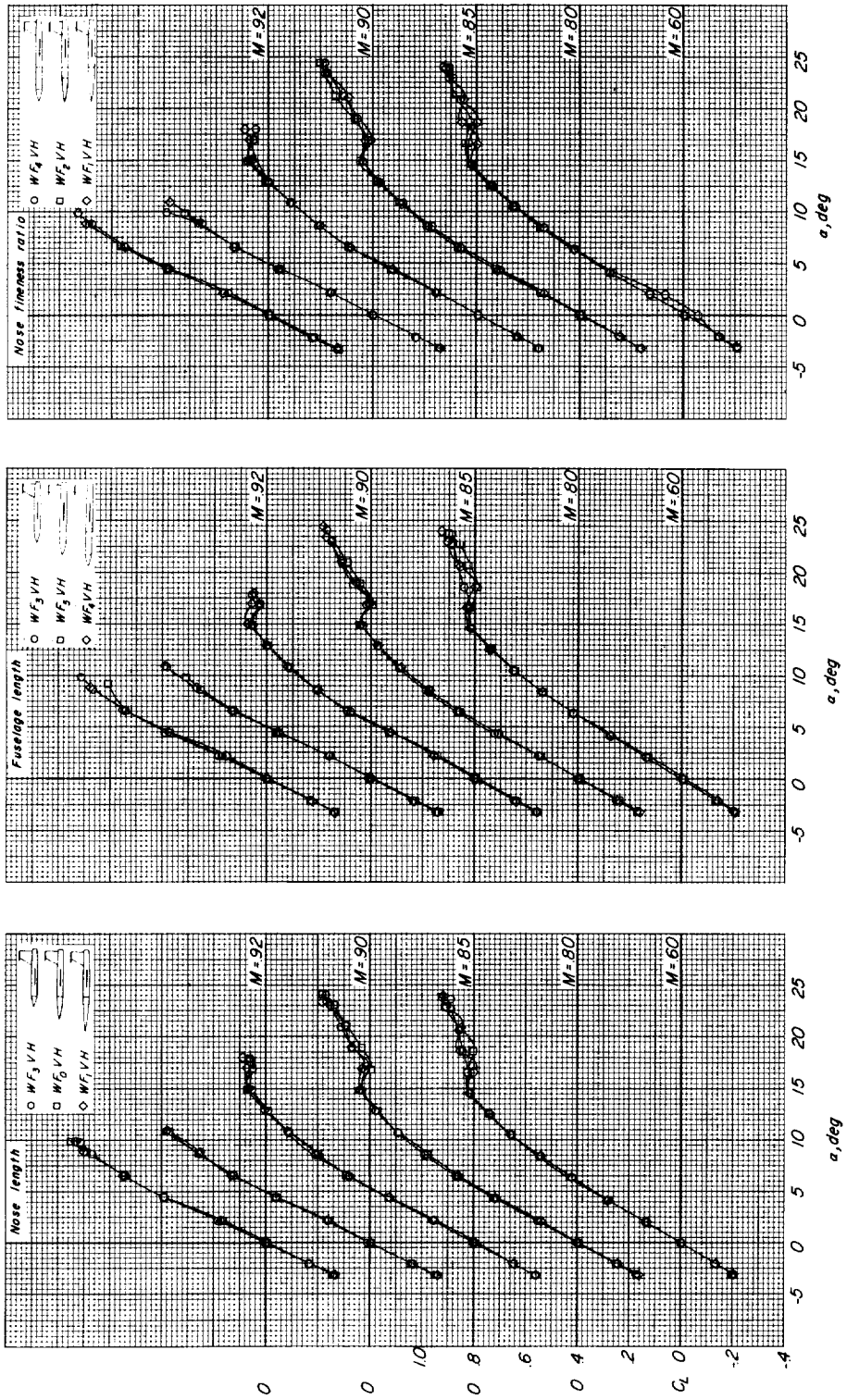

(c) C_L against α.

Figure 10.- Continued.

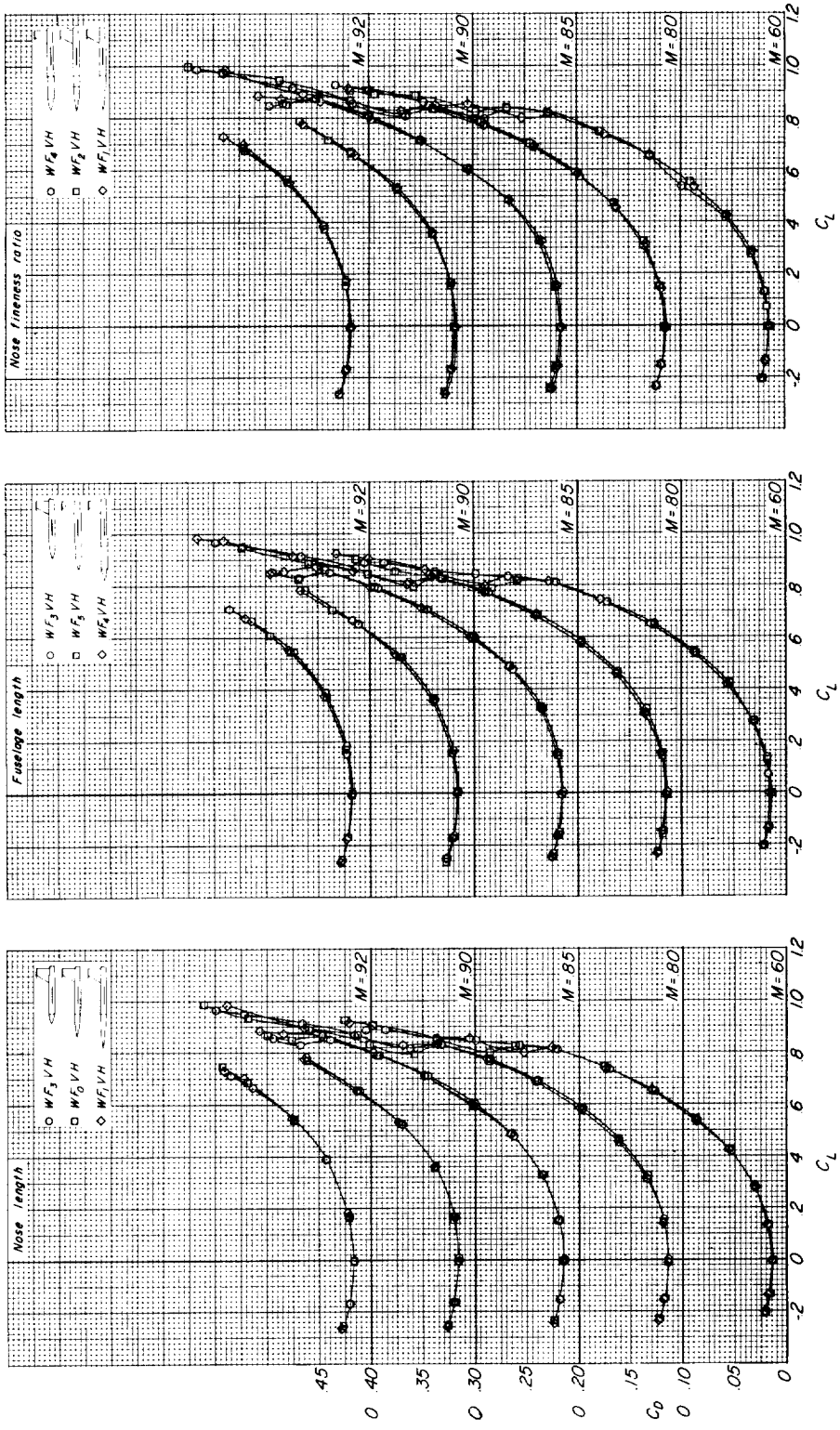

(d) C_D against C_L.

Figure 10.- Concluded.

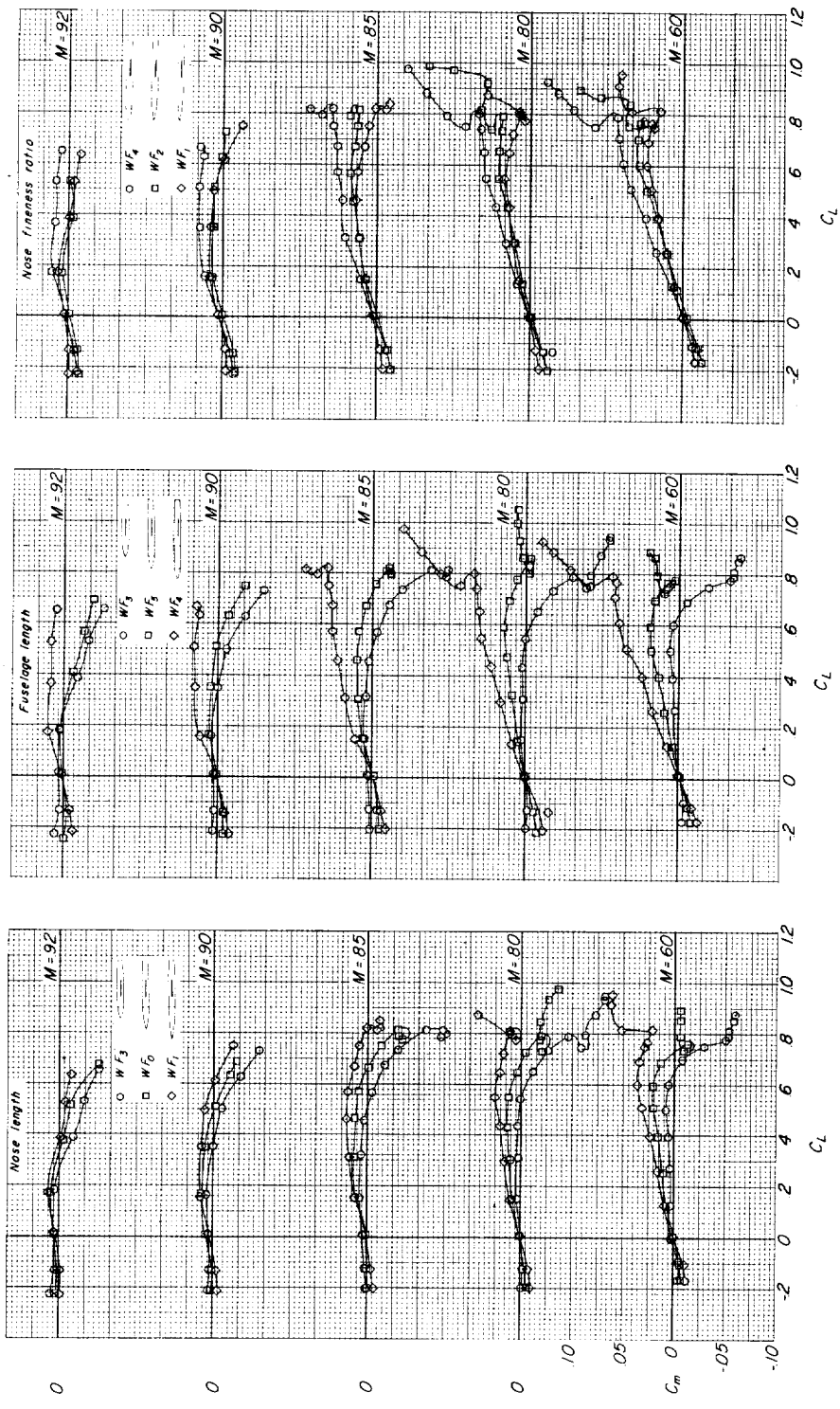

(a) C_m against C_L.

Figure 11.- Effect of nose length, fuselage length, and nose fineness ratio on the longitudinal aerodynamic characteristics of a highly tapered wing model. Tail off.

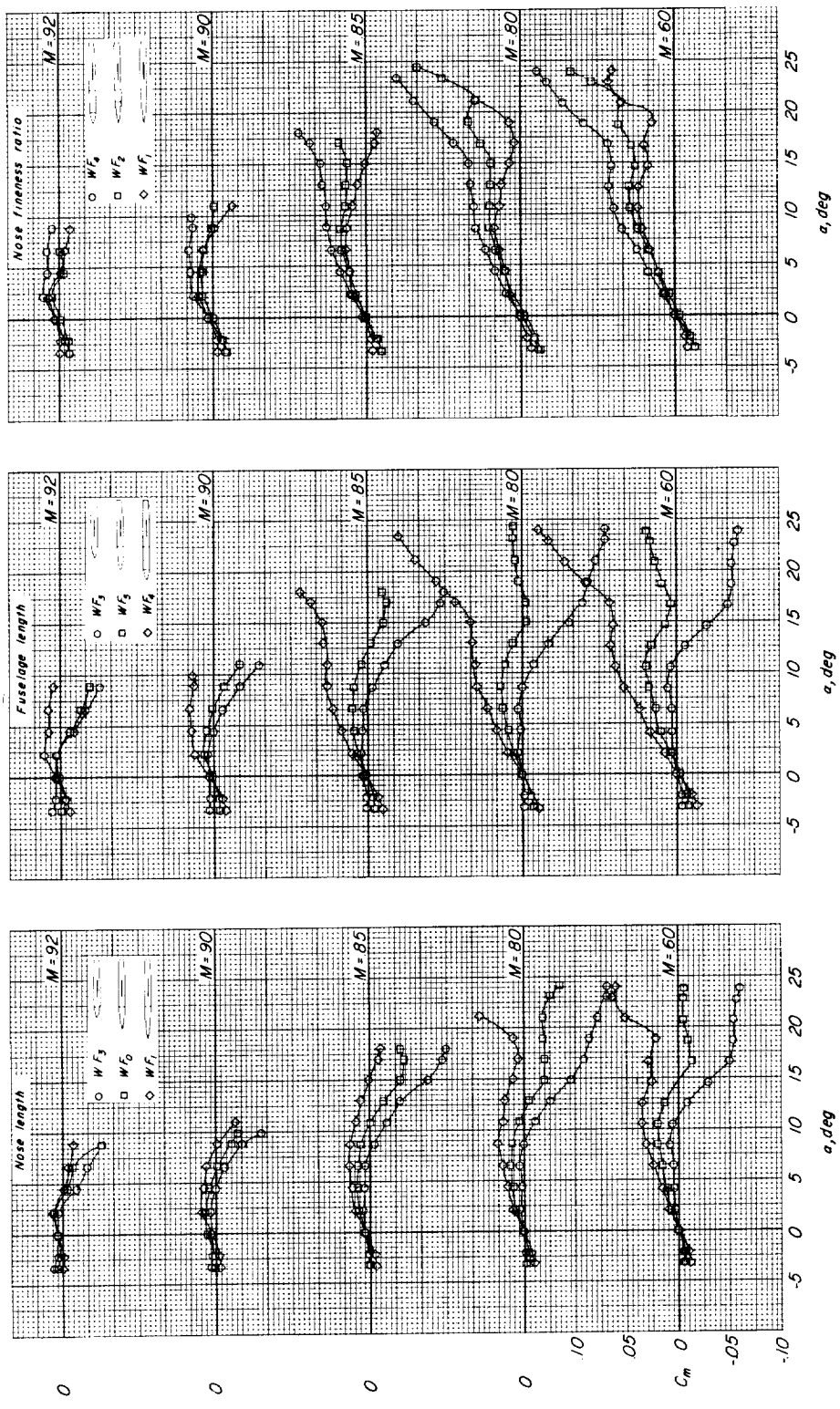

(b) C_m against α.

Figure 11.- Continued.

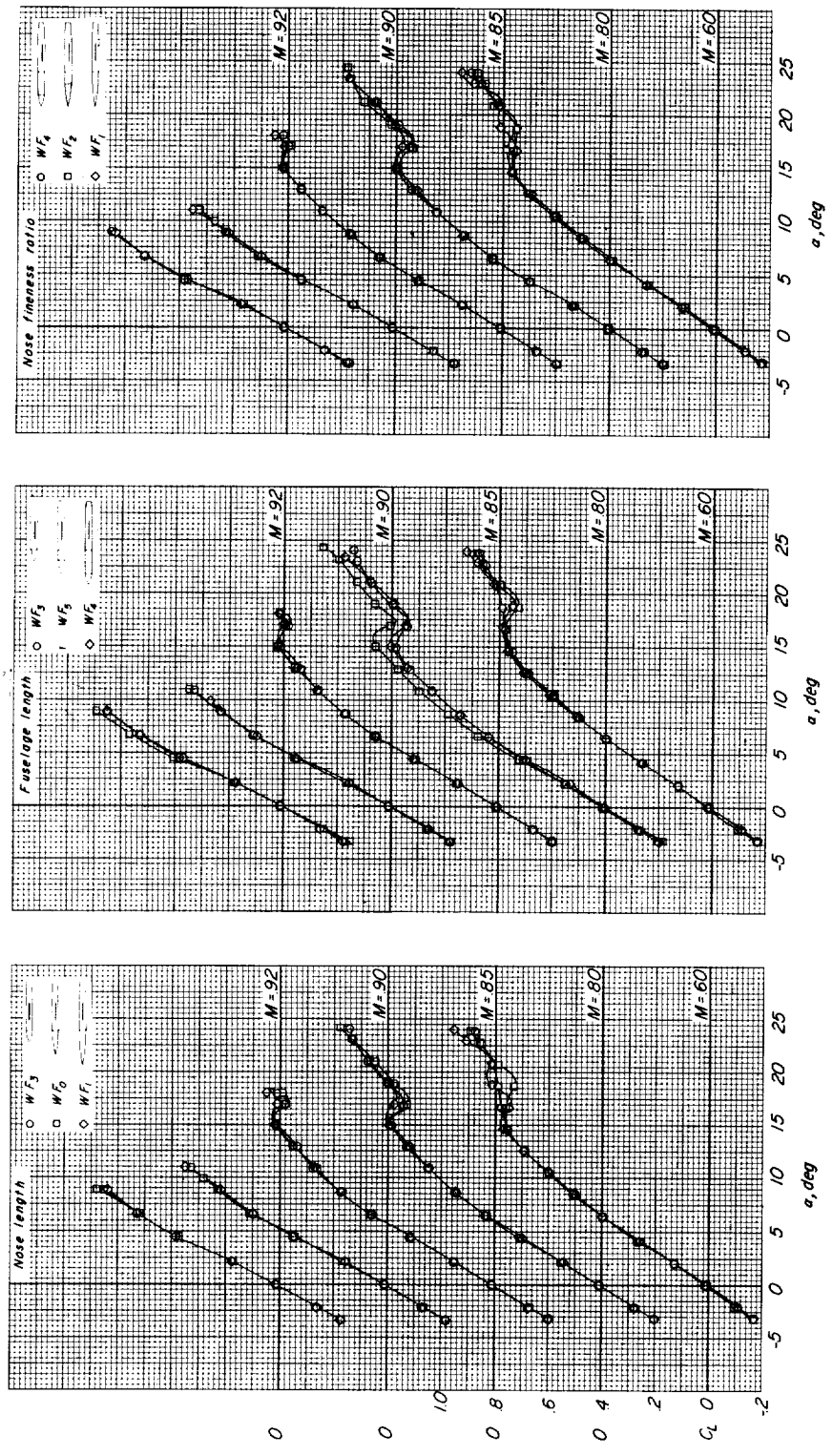

(c) C_L against α.

Figure 11.- Continued.

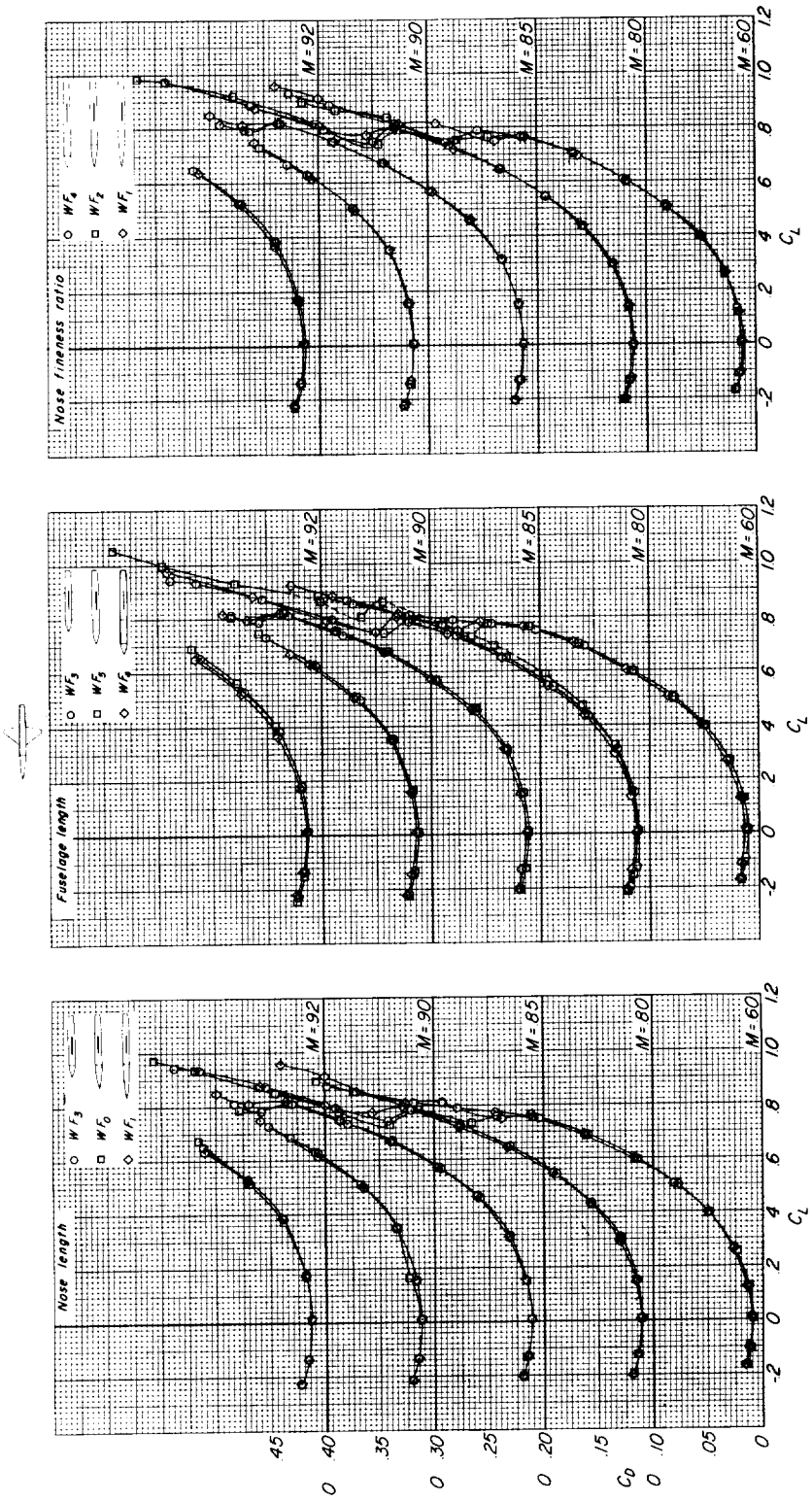

(d) C_D against C_L.

Figure 11.- Concluded.

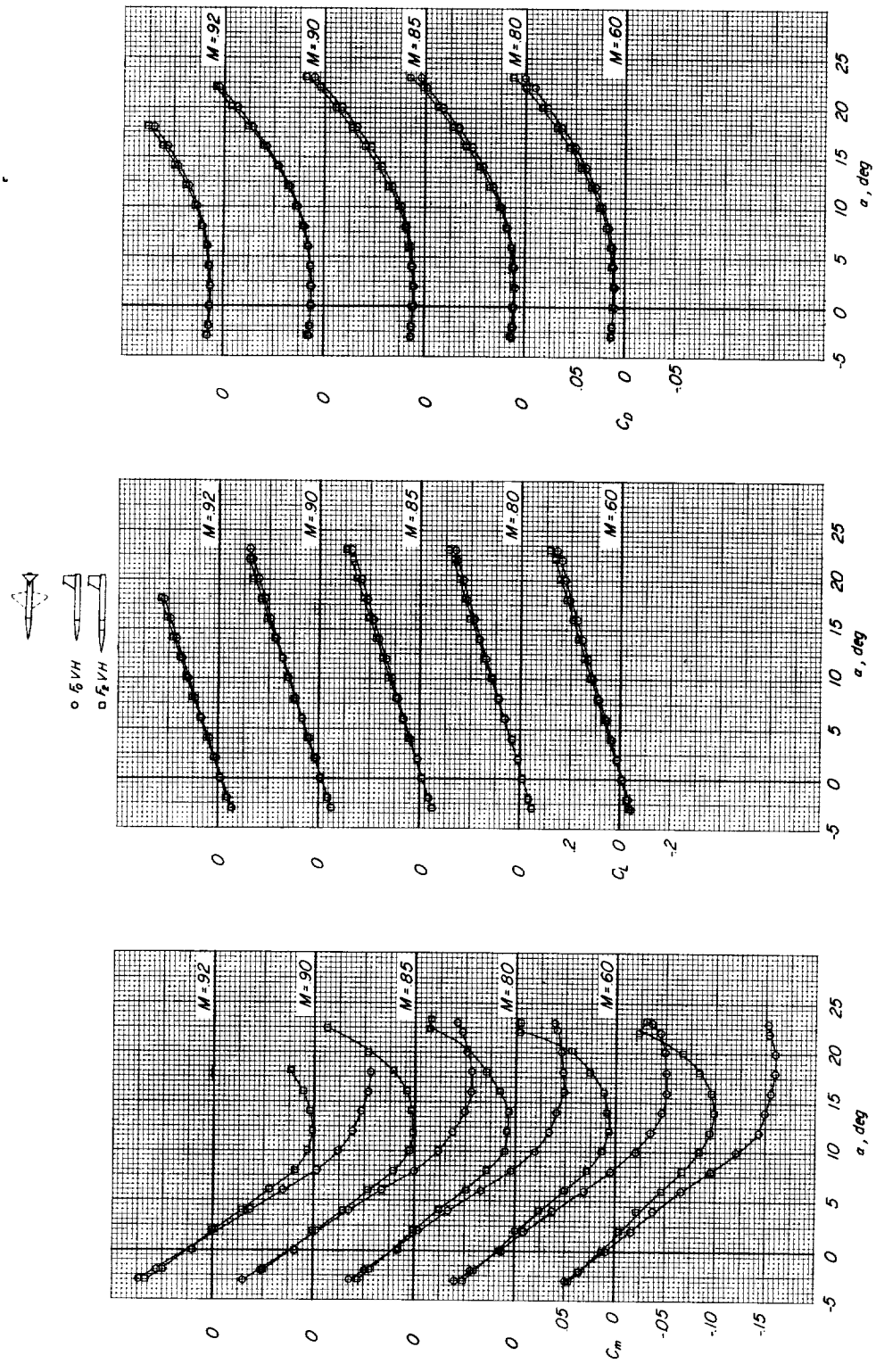

Figure 12.- Effect of nose length on the longitudinal characteristics of the fuselage and tail of the highly tapered wing model. T-tail.

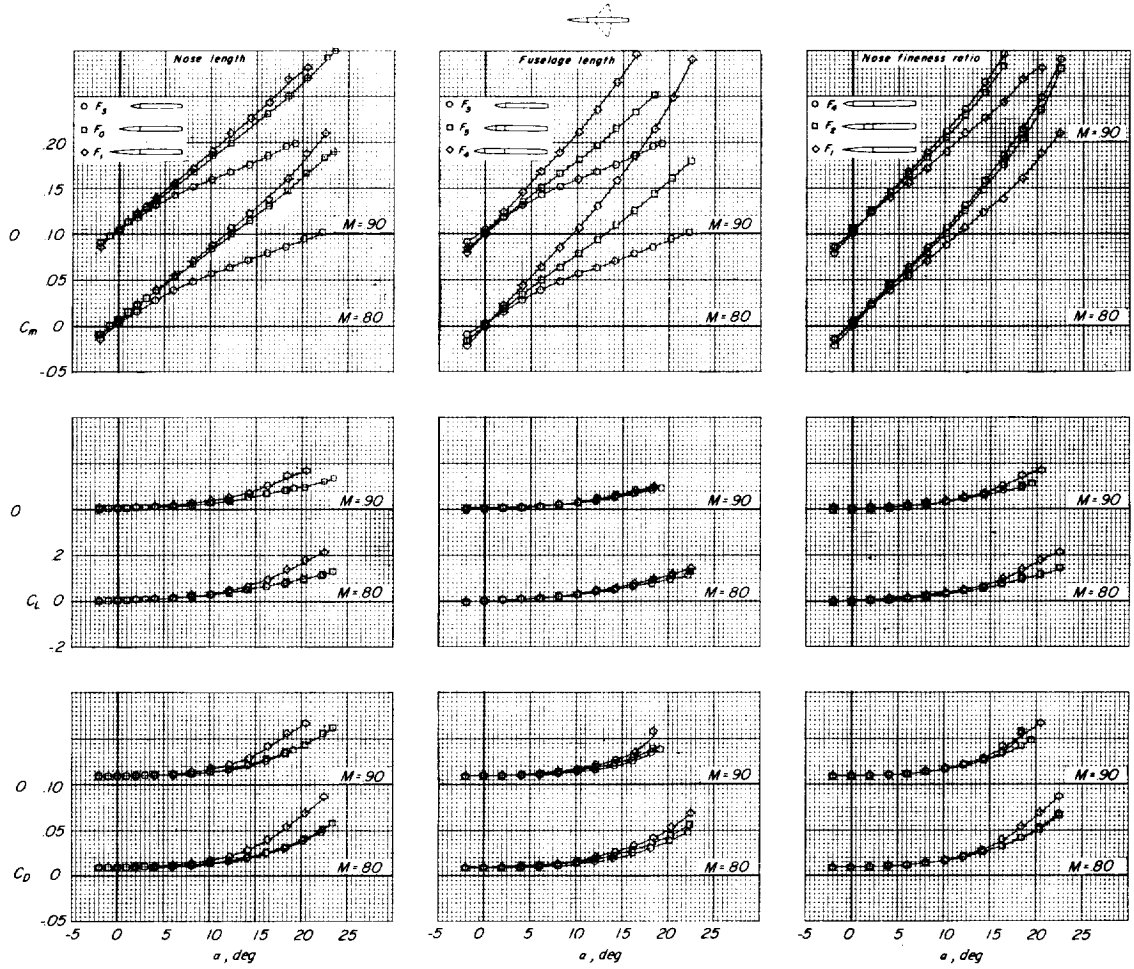

Figure 13.- Effect of nose length, fuselage length, and nose fineness ratio on the longitudinal characteristics of the fuselage of the highly tapered wing model.

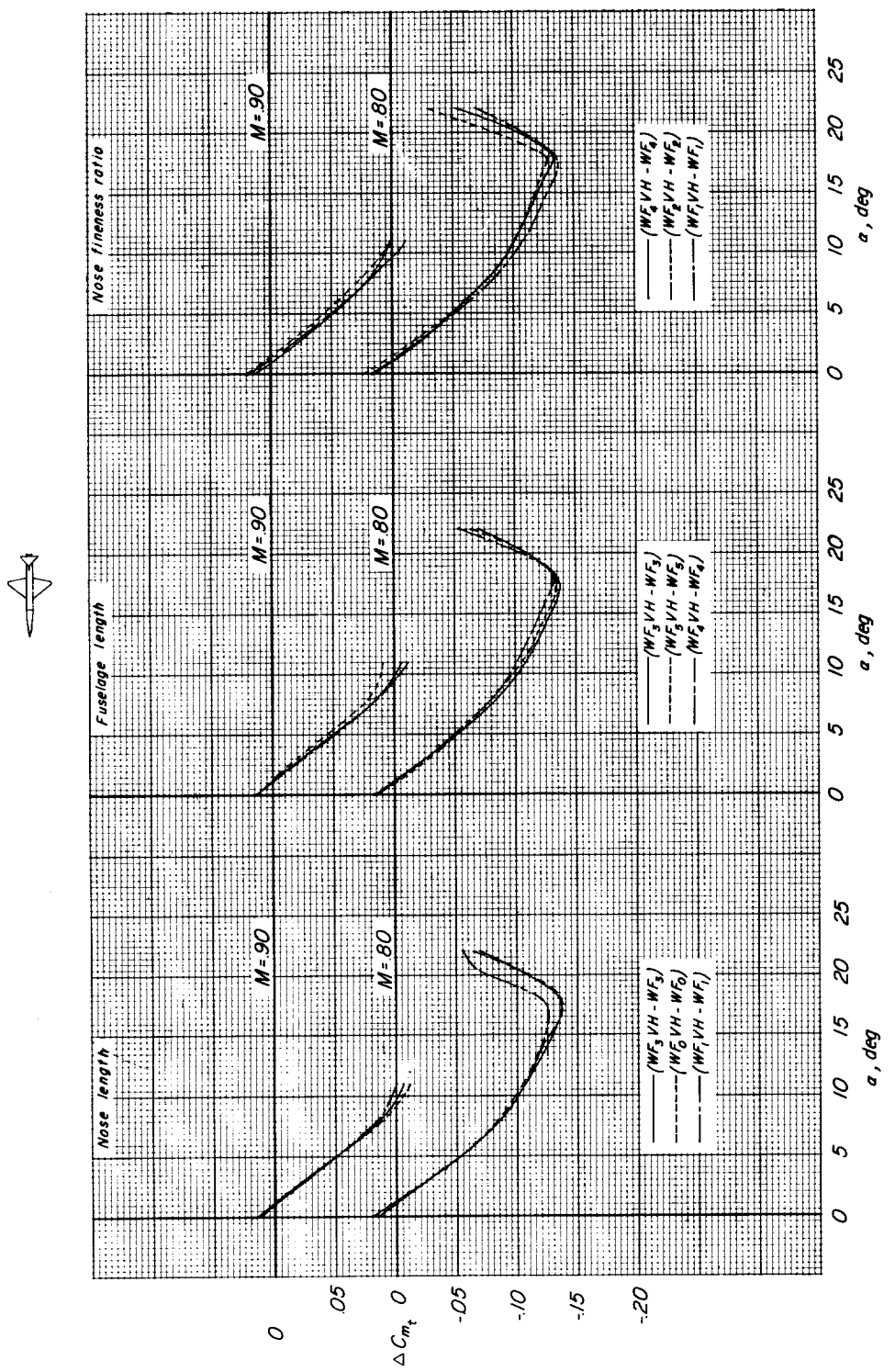

(a) Wing on.

Figure 14.- Effect of nose length, fuselage length, and nose fineness ratio on the tail contribution to the highly tapered wing model. T-tail.

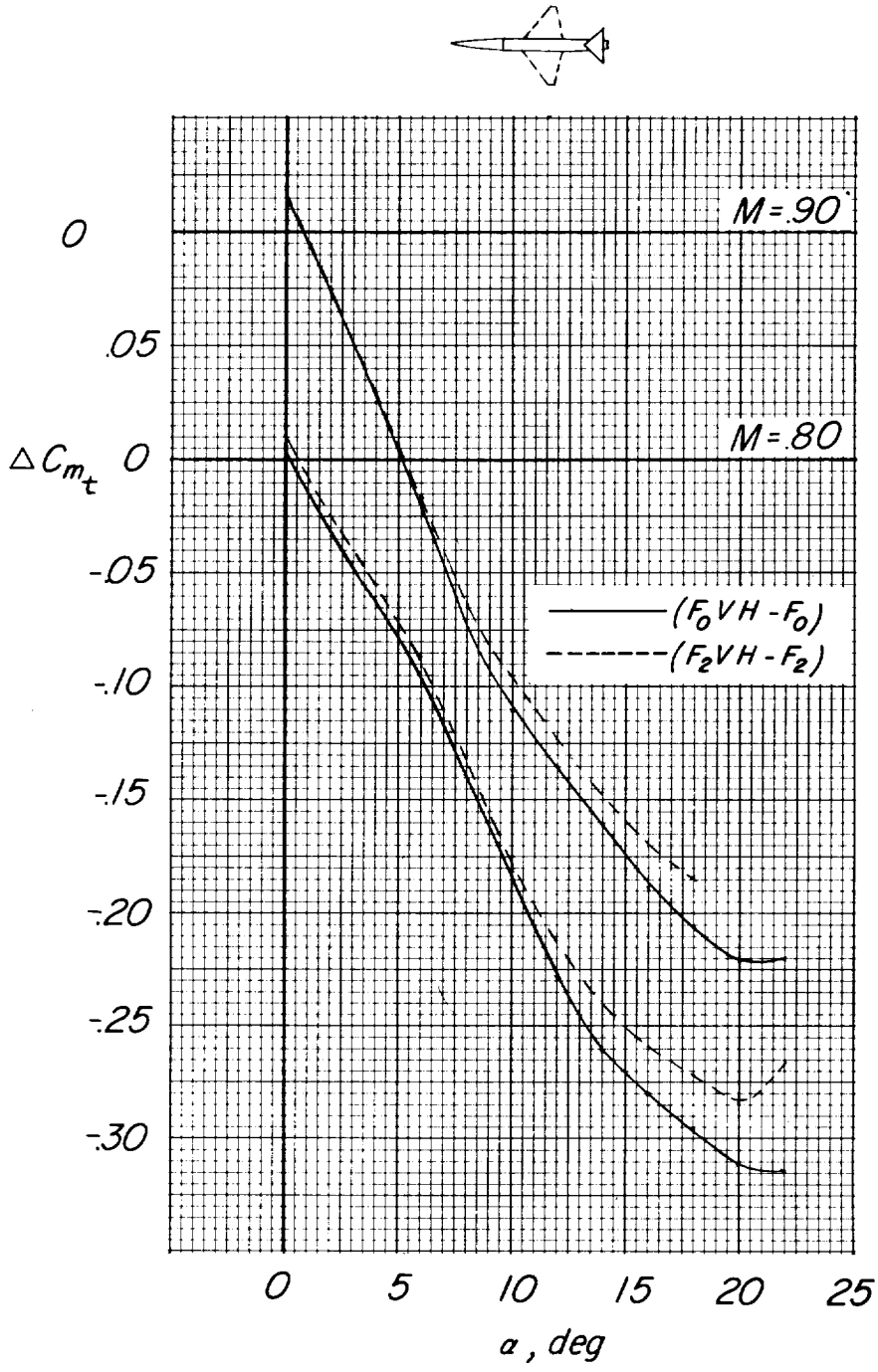

(b) Wing off.

Figure 14.- Concluded.

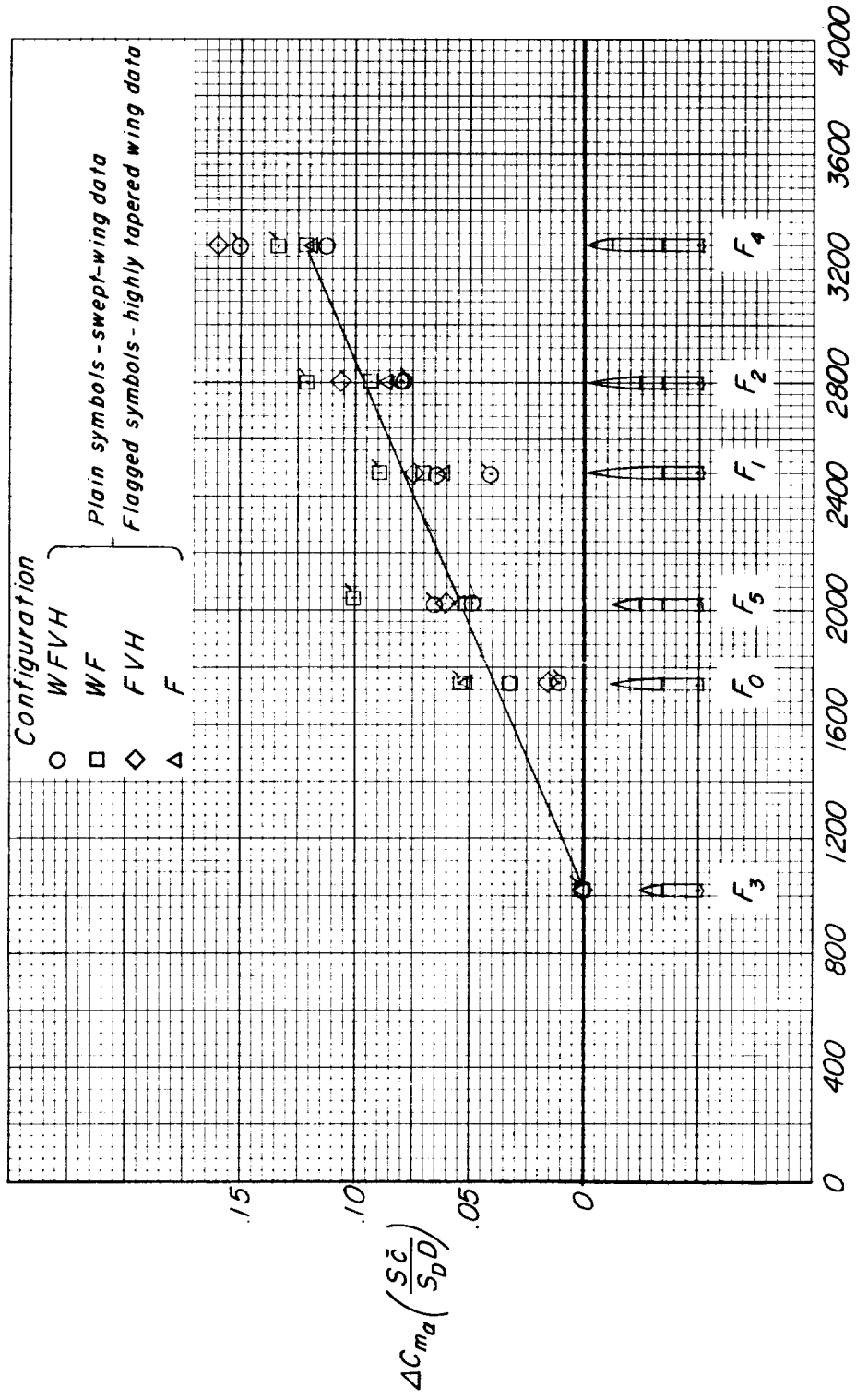

Figure 15.- Correlation of pitching-moment slope with nose moment of area.

NASA MEMO 10-10-58L
National Aeronautics and Space Administration.
EFFECT OF NOSE LENGTH, FUSELAGE LENGTH, AND NOSE FINENESS RATIO ON THE LONGITUDINAL AERODYNAMIC CHARACTERISTICS OF TWO COMPLETE MODELS AT HIGH SUBSONIC SPEEDS. Kenneth W. Goodson. October 1958. 40p. diagrs., tab. (NASA MEMO 10-10-58L)

This paper presents the results of an investigation made on a model with a swept wing and low tail and a model with a highly tapered wing of moderate sweep and a T-tail. For either the swept-wing model or the highly tapered wing model, the effects of forebody changes amounted primarily to rotations of the pitching-moment curves (changes in static margin) over the test ranges of angle of attack and Mach number. For the range of body shapes investigated the longitudinal stability at low lift is decreased by an increase in nose length or in fuselage length or by a reduction in nose fineness ratio when the fuselage length is held constant. In general, the stability for

Copies obtainable from NASA, Washington (over)

1. Wings, Complete - Sweep (1.2.2.2.3)
2. Mach Number Effects - Complete Wings (1.2.2.6)
3. Bodies - Shape Variables (1.3.2)
4. Tail-Wing-Fuselage Combinations - Airplanes (1.7.1.1.3)
5. Stability, Longitudinal - Static (1.8.1.1.1)

I. Goodson, Kenneth W.
II. NASA MEMO 10-10-58L

NASA

NASA MEMO 10-10-58L
National Aeronautics and Space Administration.
EFFECT OF NOSE LENGTH, FUSELAGE LENGTH, AND NOSE FINENESS RATIO ON THE LONGITUDINAL AERODYNAMIC CHARACTERISTICS OF TWO COMPLETE MODELS AT HIGH SUBSONIC SPEEDS. Kenneth W. Goodson. October 1958. 40p. diagrs., tab. (NASA MEMO 10-10-58L)

This paper presents the results of an investigation made on a model with a swept wing and low tail and a model with a highly tapered wing of moderate sweep and a T-tail. For either the swept-wing model or the highly tapered wing model, the effects of forebody changes amounted primarily to rotations of the pitching-moment curves (changes in static margin) over the test ranges of angle of attack and Mach number. For the range of body shapes investigated the longitudinal stability at low lift is decreased by an increase in nose length or in fuselage length or by a reduction in nose fineness ratio when the fuselage length is held constant. In general, the stability for

Copies obtainable from NASA, Washington (over)

1. Wings, Complete - Sweep (1.2.2.2.3)
2. Mach Number Effects - Complete Wings (1.2.2.6)
3. Bodies - Shape Variables (1.3.2)
4. Tail-Wing-Fuselage Combinations - Airplanes (1.7.1.1.3)
5. Stability, Longitudinal - Static (1.8.1.1.1)

I. Goodson, Kenneth W.
II. NASA MEMO 10-10-58L

NASA

NASA MEMO 10-10-58L
National Aeronautics and Space Administration.
EFFECT OF NOSE LENGTH, FUSELAGE LENGTH, AND NOSE FINENESS RATIO ON THE LONGITUDINAL AERODYNAMIC CHARACTERISTICS OF TWO COMPLETE MODELS AT HIGH SUBSONIC SPEEDS. Kenneth W. Goodson. October 1958. 40p. diagrs., tab. (NASA MEMO 10-10-58L)

This paper presents the results of an investigation made on a model with a swept wing and low tail and a model with a highly tapered wing of moderate sweep and a T-tail. For either the swept-wing model or the highly tapered wing model, the effects of forebody changes amounted primarily to rotations of the pitching-moment curves (changes in static margin) over the test ranges of angle of attack and Mach number. For the range of body shapes investigated the longitudinal stability at low lift is decreased by an increase in nose length or in fuselage length or by a reduction in nose fineness ratio when the fuselage length is held constant. In general, the stability for

Copies obtainable from NASA, Washington (over)

1. Wings, Complete - Sweep (1.2.2.2.3)
2. Mach Number Effects - Complete Wings (1.2.2.6)
3. Bodies - Shape Variables (1.3.2)
4. Tail-Wing-Fuselage Combinations - Airplanes (1.7.1.1.3)
5. Stability, Longitudinal - Static (1.8.1.1.1)

I. Goodson, Kenneth W.
II. NASA MEMO 10-10-58L

NASA

NASA MEMO 10-10-58L
National Aeronautics and Space Administration.
EFFECT OF NOSE LENGTH, FUSELAGE LENGTH, AND NOSE FINENESS RATIO ON THE LONGITUDINAL AERODYNAMIC CHARACTERISTICS OF TWO COMPLETE MODELS AT HIGH SUBSONIC SPEEDS. Kenneth W. Goodson. October 1958. 40p. diagrs., tab. (NASA MEMO 10-10-58L)

This paper presents the results of an investigation made on a model with a swept wing and low tail and a model with a highly tapered wing of moderate sweep and a T-tail. For either the swept-wing model or the highly tapered wing model, the effects of forebody changes amounted primarily to rotations of the pitching-moment curves (changes in static margin) over the test ranges of angle of attack and Mach number. For the range of body shapes investigated the longitudinal stability at low lift is decreased by an increase in nose length or in fuselage length or by a reduction in nose fineness ratio when the fuselage length is held constant. In general, the stability for

Copies obtainable from NASA, Washington (over)

1. Wings, Complete - Sweep (1.2.2.2.3)
2. Mach Number Effects - Complete Wings (1.2.2.6)
3. Bodies - Shape Variables (1.3.2)
4. Tail-Wing-Fuselage Combinations - Airplanes (1.7.1.1.3)
5. Stability, Longitudinal - Static (1.8.1.1.1)

I. Goodson, Kenneth W.
II. NASA MEMO 10-10-58L

NASA

NASA MEMO 10-10-58L

all model configurations showed substantially the same variation with changes in forebody area of moment.

Copies obtainable from NASA, Washington

NASA

NASA MEMO 10-10-58L

all model configurations showed substantially the same variation with changes in forebody area of moment.

Copies obtainable from NASA, Washington

NASA

NASA MEMO 10-10-58L

all model configurations showed substantially the same variation with changes in forebody area of moment.

Copies obtainable from NASA, Washington

NASA

NASA MEMO 10-10-58L

all model configurations showed substantially the same variation with changes in forebody area of moment.

Copies obtainable from NASA, Washington

NASA